

Figure 114: Representative chromatograms for Type IIIB waxy bitumen. (A) Whole-oil GC-MS TIC showing alkane distribution. (B) m/z 191 chromatogram showing distribution of terpanes. (C) m/z 217 chromatogram showing distribution of steranes and diasteranes. (D) m/z 218 chromatogram showing distribution of C27-C29 $\alpha\beta$ steranes. (E) m/z 259 chromatogram showing distribution of C27-C29 $\beta\alpha$ diasteranes and TPP. For peak identifications refer to tables 18 and 19.

Type IIIC waxy bitumens

Representative chromatograms for Type IIIC waxy bitumens are shown in Figure 115. Preliminary assessment of the biomarker compounds identified by TIC GC-MS, SIM GC-MS and MRM GC-MS-MS for the least altered specimens (summarised in Table 29) suggest they are derived from a lacustrine shale deposited under sub-oxic conditions. The absence of gammacerane and lower C_{26}/C_{25} tricyclic terpane ratio distinguish this sub-family from Type IIIA.

The presence of bicadinanes, oleanane and tetracyclic polyprenoids supports the interpretation that these bitumens are derived from an Indonesian source rock of Cenozoic age.

Table 29: Summary of source characteristics and key features of Type IIIC waxy bitumens.

| Oil Family | Source Characteristics | Key Features |
|---------------------------|--|---|
| Type IIIC waxy bitumen | Lacustrine shale deposited in sub-oxic conditions Presence of bicadinanes, oleanane supports Indonesian Cenozoic origin | Pr/Ph = 1.8-1.9 |
| | | Botryococcane absent |
| | | C_{27}/C_{29} sterane >1 |
| | | 24- <i>n</i> -propylcholestane absent/trace |
| | | C_{30} 4-Me sterane > C_{29} sterane |
| | | C_{27} dia/(dia+reg) sterane = 0.49 |
| | | C_{26}/C_{25} tricyclic terpane = 1.53 |
| | | C_{29}/C_{30} $\alpha\beta$ hopane = 0.73 |
| | | C_{35}/C_{34} homohopane = 0.42 |
| | | C_{35} homohopane index = 0.05 |
| | | Gammacerane absent |
| | | Oleanane (low) |
| | | Bicadinanes |
| | | TPP (high) |

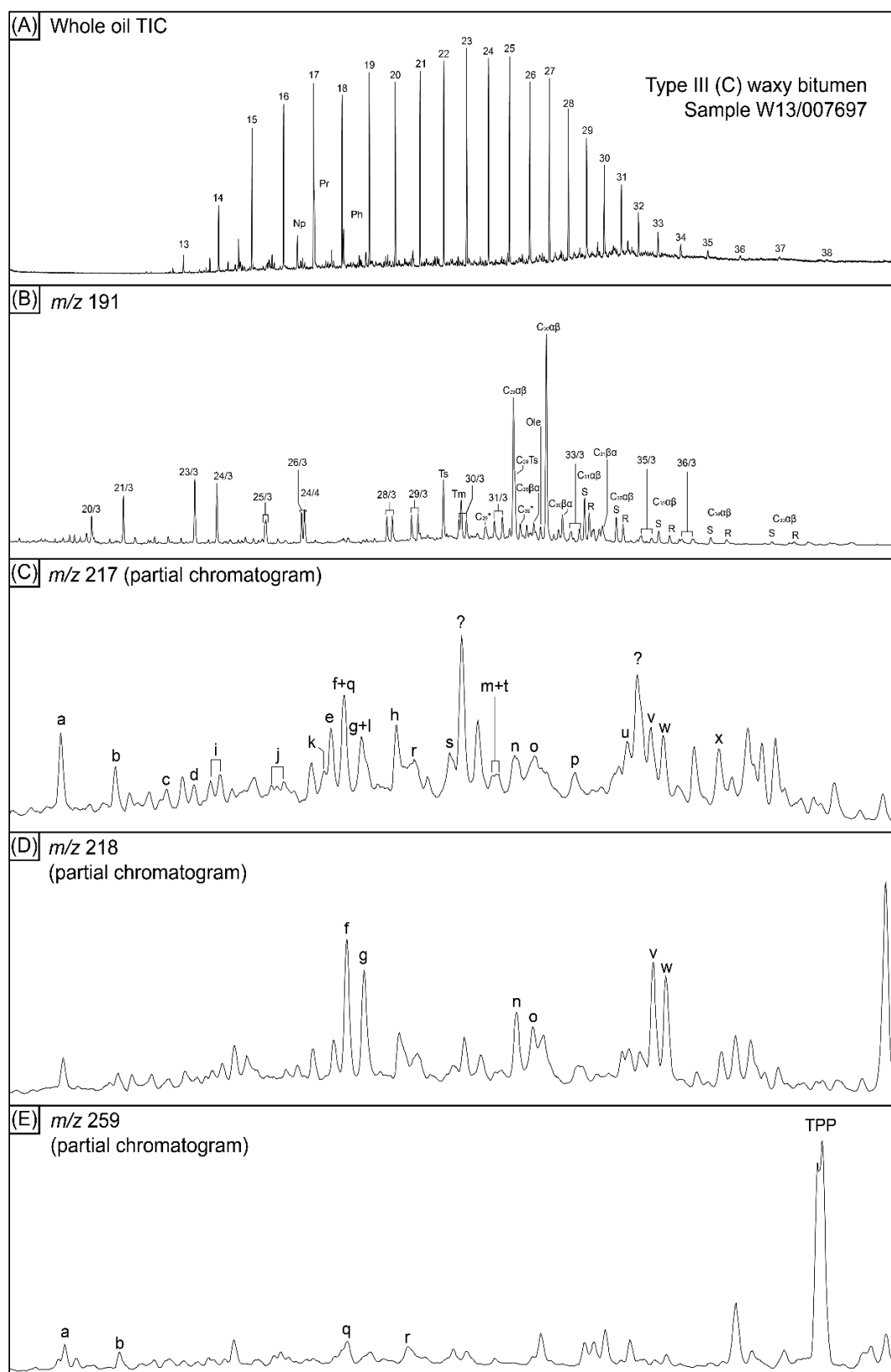


Figure 115: Representative chromatograms for Type III (C) waxy bitumen. (A) Whole-oil GC-MS TIC showing alkane distribution. (B) m/z 191 chromatogram showing distribution of terpanes. (C) m/z 217 chromatogram showing distribution of steranes and diasteranes. (D) m/z 218 chromatogram showing distribution of C27-C29 $\alpha\beta$ steranes. (E) m/z 259 chromatogram showing distribution of C27-C29 $\beta\alpha$ diasteranes and TPP. For peak identifications refer to tables 18 and 19.

Type IIID waxy bitumens

Representative chromatograms for Type IIID waxy bitumen are shown in Figure 116. Preliminary assessment of the biomarker compounds identified by TIC GC-MS, SIM GC-MS and MRM GC-MS-MS for the least altered specimens (summarised in Table 30) suggest them to be derived from a deltaic shale (or migrated through a delta) with terrestrial organic matter input.

The presence of bisnorlupanes is consistent with a Cenozoic Indonesian origin, potentially in the offshore Kutei Basin.

Table 30: Summary of source characteristics and key features of Type IIID waxy bitumens.

| Oil Family | Source Characteristics | Key Features |
|------------------------|---|--|
| Type IIID waxy bitumen | Cenozoic deltaic shale (or migrated through a Cenozoic delta) with terrestrial organic matter input. | Pr/Ph altered/removed (biodegradation) |
| | | Botryococcane absent |
| | Presence of bisnorlupanes is consistent with an Indonesian origin, potentially the offshore Kutei Basin (Curiale et al., 2005, 2006), or the Misool seafloor seep (Noble et al., 2009). | C_{27}/C_{29} sterane <1 (possible artefact of severe biodegradation) |
| | | 24- <i>n</i> -propylcholestane absent/trace |
| | | C_{30} 4-Me sterane < C_{29} sterane |
| | | C_{27} dia/(dia+reg) sterane = 0.30 |
| | | C_{26}/C_{25} tricyclic terpane = 1.25 |
| | | C_{29}/C_{30} $\alpha\beta$ hopane = 0.53 |
| | | C_{35}/C_{34} homohopane = 0.43 |
| | | C_{35} homohopane index = 0.03 |
| | | Gammacerane |
| | | Oleanane (high) |
| | | Bicadinanes (high) |
| | | TPP low |
| | | Bisnorlupanes, bisnoroleanane & taraxastane |

Type III E waxy bitumens

Representative chromatograms for Type III E waxy bitumen are shown in Figure 117. Preliminary assessment of the biomarker compounds identified by TIC GC-MS, SIM GC-MS and MRM GC-MS-MS for the key specimens (summarised in Table 31) suggest they are derived from a lacustrine shale with terrestrial organic matter input.

The saturate fractions of samples assigned to this sub-family gave very low yields and provided poor data quality with potentially inaccurate ratios. As such, this bitumen is currently of unknown origin.

Table 31: Summary of source characteristics and key features of Type III E waxy bitumens.

| Oil Family | Source Characteristics | Key Features |
|----------------------------|---|--|
| Type III E waxy bitumen | Lacustrine shale with terrestrial organic matter input. | Pr/Ph absent (biodegradation) |
| | | Botryococcane absent |
| | | C_{27}/C_{29} sterane >1 |
| | | 24- <i>n</i> -propylcholestane absent/trace |
| | * Ratios may be inaccurate due to poor data quality. Re-analysis in progress to confirm. | C_{30} 4-Me sterane < C_{29} sterane |
| | | C_{27} dia/(dia+reg) sterane = 0.69 |
| | Origin unknown | C_{26}/C_{25} tricyclic terpane = 1.51* |
| | | C_{29}/C_{30} $\alpha\beta$ hopane = 0.64* |
| | | C_{35}/C_{34} homohopane = 0.78* |
| | | C_{35} homohopane index = 0.07* |
| | | Gammacerane (low) |
| | | Oleanane (low) |
| | | Bicadinanes (high) |
| | | TPP (low) |

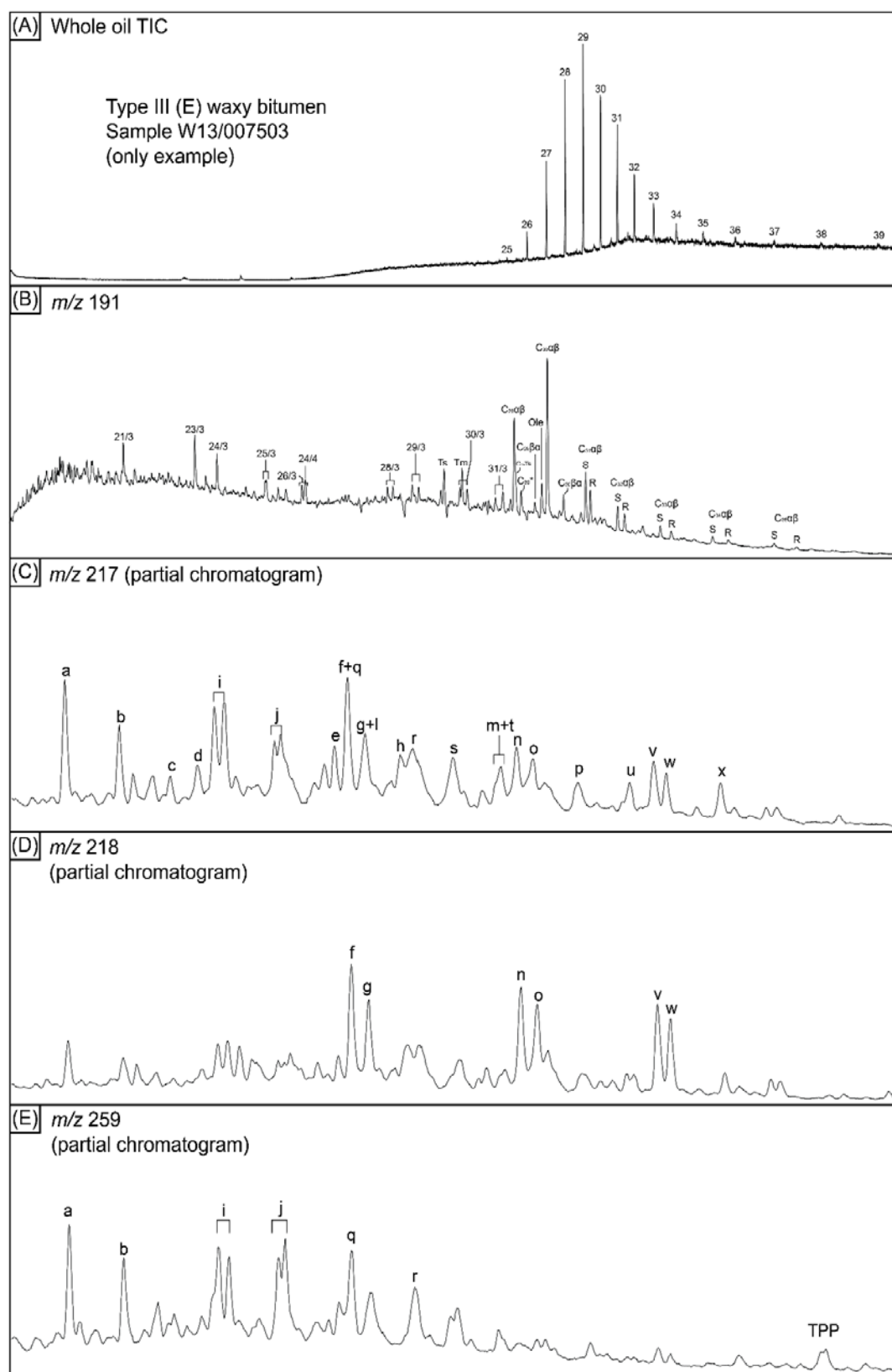


Figure 117: Representative chromatograms for Type III E waxy bitumen. (A) Whole-oil GC-MS TIC showing alkane distribution. (B) m/z 191 chromatogram showing distribution of terpanes. (C) m/z 217 chromatogram showing distribution of steranes and diasteranes. (D) m/z 218 chromatogram showing distribution of C27-C29 $\alpha\beta$ steranes. (E) m/z 259 chromatogram showing distribution of C27-C29 $\beta\alpha$ diasteranes and TPP. For peak identifications refer to tables 18 and 19.

Type IV Waxy Bitumens (No Botryococcane, High Wax)

Type IV waxy bitumens are characterised by their lack of botryococcane and high abundances of waxy *n*-alkanes (C₃₅–C₃₉).

Biomarker analysis (discussed below) demonstrates five potential oil families exist within the whole oil category of Type IV waxy bitumen. Although pristane and phytane are intact in certain samples, they were depleted in others and could not be used in any interpretations of source conditions or for correlation purposes.

Type IVA waxy bitumens

Representative chromatograms for Type IVA waxy bitumen are shown in Figure 118. Preliminary assessment of the biomarker compounds identified by TIC GC-MS, SIM GC-MS and MRM GC-MS-MS for the least altered specimens (summarised in Table 32) suggest they are derived from a source rock of sub-oxic brackish/lacustrine affinity.

The absence of botryococcane, oleanane and bicadinanes precludes an Indonesian origin.

Table 32: Summary of source characteristics and key features of Type IVA waxy bitumen.

| Oil Family | Source Characteristics | Key Features |
|--------------------------|--|---|
| Type IVA waxy bitumen | Known parameters suggest a sub-oxic brackish/lacustrine source. | Pr/Ph = 1.25 (potentially slight alteration) |
| | | Botryococcane absent |
| | *Confirmation of presence of 24- <i>n</i> -propylcholestane is required. | C ₂₇ /C ₂₉ sterane >1 |
| | | 24- <i>n</i> -propylcholestane TBD* |
| | Absence of oleanane and bicadinanes precludes Indonesian origin | C ₃₀ 4-Me sterane < C ₂₉ sterane |
| | | C ₂₇ dia/(dia+reg) sterane = 0.68 |
| | | C ₂₆ /C ₂₅ tricyclic terpane = 1.34 |
| | | C ₂₉ /C ₃₀ αβ hopane = 0.61 |
| | | C ₃₅ /C ₃₄ homohopane = 0.67 |
| | | C ₃₅ homohopane index = 0.07 |
| | | Gammacerane |
| | | Oleanane absent |
| | | Bicadinanes absent |
| | | TPP (low) |

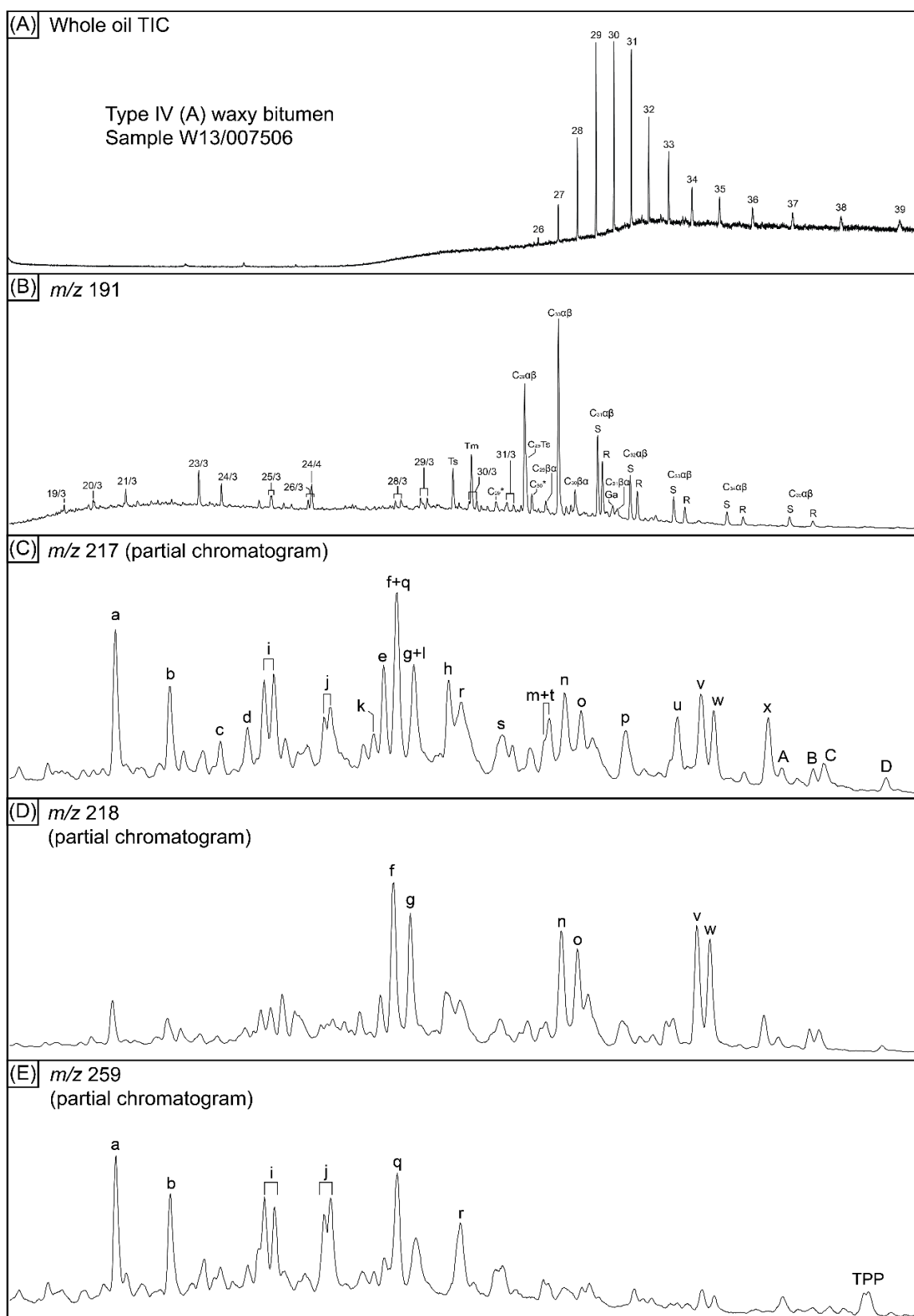


Figure 118: Representative chromatograms for Type IVA waxy bitumen. (A) Whole-oil GC-MS TIC showing alkane distribution. (B) m/z 191 chromatogram showing distribution of terpanes. (C) m/z 217 chromatogram showing distribution of steranes and diasteranes. (D) m/z 218 chromatogram showing distribution of C_{27} - C_{29} $\alpha\beta$ steranes. (E) m/z 259 chromatogram showing distribution of C_{27} - C_{29} $\beta\alpha$ diasteranes and TPP. For peak identifications refer to tables 18 and 19.

Type IVB waxy bitumens

Representative chromatograms for Type IVB waxy bitumen are shown in Figure 119. Preliminary assessment of the biomarker compounds identified by TIC GC-MS, SIM GC-MS and MRM GC-MS-MS for the least altered specimens (summarised in Table 33) suggest they are derived from a deltaic shale with terrestrial organic matter input (or that they have subsequently migrated through a deltaic sequence).

The presence of oleanane, bicadinanes and bisnorlupanes is consistent with a Cenozoic Indonesian origin, potentially in the offshore Kutei Basin.

Table 33: Summary of source characteristics and key features of Type IVB waxy bitumens.

| Oil Family | Source Characteristics | Key Features |
|-----------------------|---|---|
| Type IVB waxy bitumen | Cenozoic deltaic shale with terrestrial organic matter input (or migrated through a Cenozoic delta) | Pr/Ph absent (biodegradation) |
| | | Botryococcane absent |
| | | C_{27}/C_{29} sterane <1 |
| | | 24- <i>n</i> -propylcholestane |
| | Presence of oleanane, bicadinanes & bisnorlupanes is consistent with an Indonesian origin. Potentially the offshore Kutei Basin (Curiale et al., 2005, 2006), or the Misool seafloor seep (Noble et al., 2009). | C_{30} 4-Me sterane < C_{29} sterane |
| | | C_{27} dia/(dia+reg) sterane = 0.40 |
| | | C_{26}/C_{25} tricyclic terpane = 0.79 |
| | | C_{29}/C_{30} $\alpha\beta$ hopane = 0.73 |
| | | C_{35}/C_{34} homohopane = 0.84 |
| | | C_{35} homohopane index = 0.06 |
| | | Gammacerane |
| | | Oleanane (high) |
| | | Bicadinanes (high) |
| | | TPP (low) |
| | | Bisnorlupanes, bisnoroleanane & taraxastane |

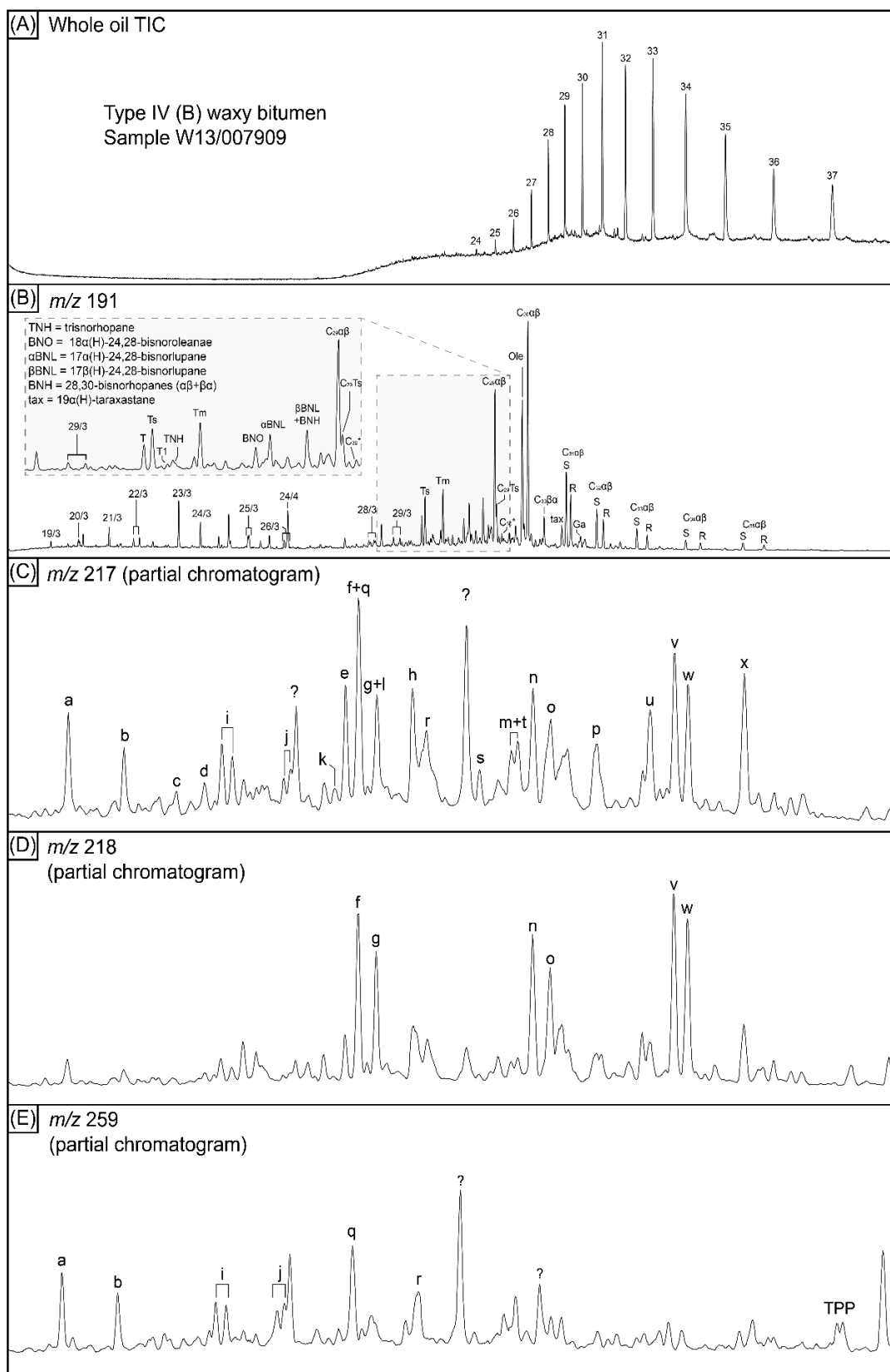


Figure 119: Representative chromatograms for Type IVB waxy bitumen. (A) Whole-oil GC-MS TIC showing alkane distribution. (B) m/z 191 chromatogram showing distribution of terpanes. (C) m/z 217 chromatogram showing distribution of steranes and diasteranes. (D) m/z 218 chromatogram showing distribution of C27-C29 $\alpha\beta$ steranes. (E) m/z 259 chromatogram showing distribution of C27-C29 $\beta\alpha$ diasteranes and TPP. For peak identifications refer to tables 18 and 19.

Type IVC waxy bitumens

Representative chromatograms for Type IVC waxy bitumens are shown in Figure 120. Preliminary assessment of the biomarker compounds identified by TIC GC-MS, SIM GC-MS and MRM GC-MS-MS for the least altered specimens (summarised in Table 34) identified they are a separate oil family on the basis of visual interpretation of the chromatograms.

The saturate fractions for samples assigned to this sub-family were obtained in very low yield and provided poor quality data with potentially inaccurate ratios. As such, this bitumen family is currently of unknown origin.

Table 34: Summary of source characteristics and key features of Type IVC waxy bitumen.

| Oil Family | Source Characteristics | Key Features |
|--------------------------|---|---|
| Type IVC waxy bitumen | Identified as separate oil family on basis of visual interpretation of chromatograms. | Pr/Ph absent (biodegradation) |
| | | Botryococcane absent |
| | | C_{27}/C_{29} sterane ≥ 1 |
| | Geochemical ratios not yet calculated. | 24- <i>n</i> -propylcholestane absent/trace |
| | | C_{30} 4-Me sterane $> C_{29}$ sterane |
| | Interpretation yet to be determined (TBD). | C_{27} dia/(dia+reg) sterane = TBD |
| | | C_{26}/C_{25} tricyclic terpane = TBD |
| | | C_{29}/C_{30} $\alpha\beta$ hopane = TBD |
| | | C_{35}/C_{34} homohopane = TBD |
| | | C_{35} homohopane index = TBD |
| | | Gammacerane = TBD |
| | | Oleanane (moderate) |
| | | Bicadinanes (high) |
| | | TPP high (potentially misleading if diasteranes are degraded) |

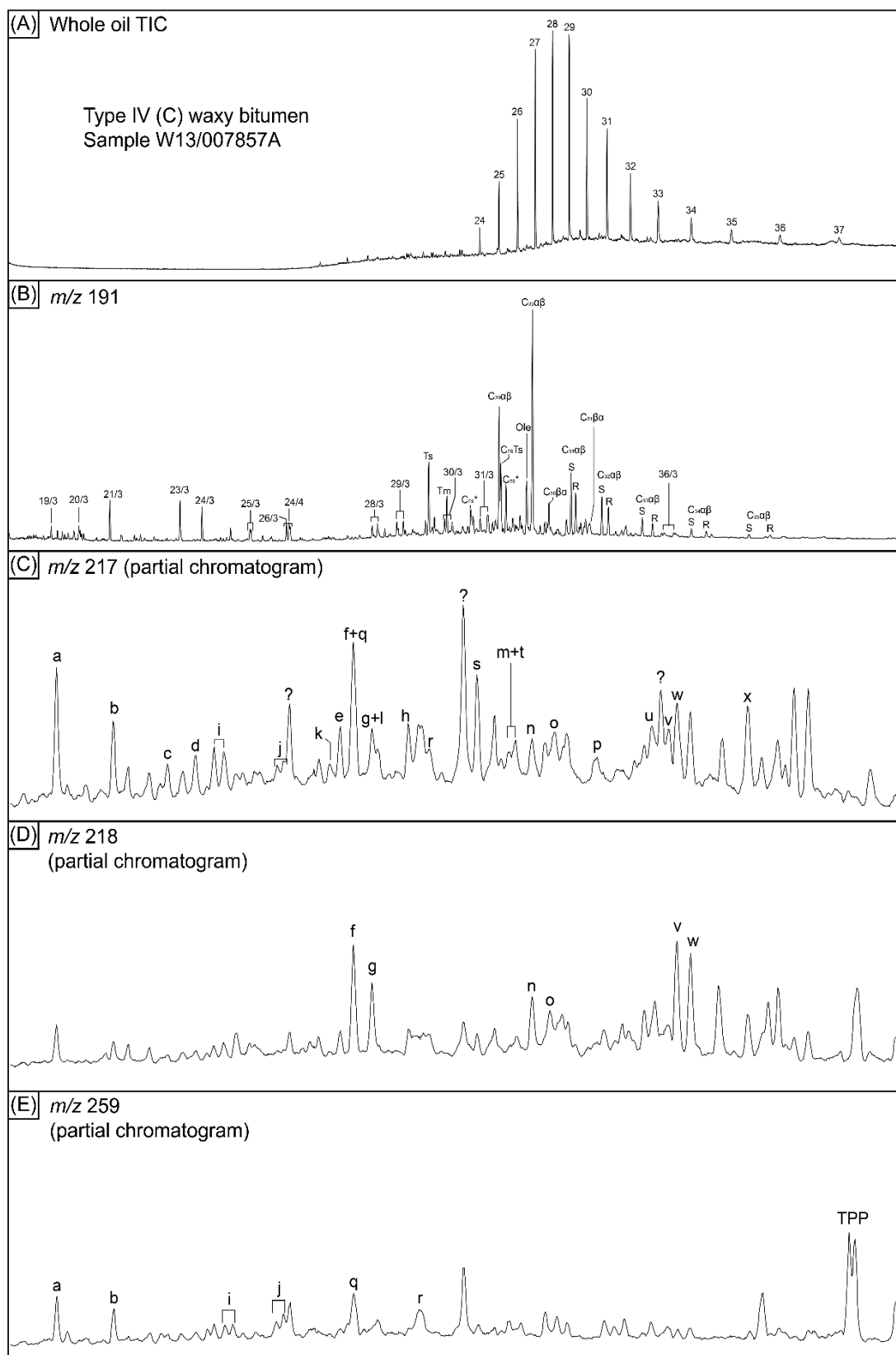


Figure 120: Representative chromatograms for Type IVC waxy bitumen. (A) Whole-oil GC-MS TIC showing alkane distribution. (B) m/z 191 chromatogram showing distribution of terpanes. (C) m/z 217 chromatogram showing distribution of steranes and diasteranes. (D) m/z 218 chromatogram showing distribution of C27-C29 $\alpha\beta$ steranes. (E) m/z 259 chromatogram showing distribution of C27-C29 $\beta\alpha$ diasteranes and TPP. For peak identifications refer to tables 18 and 19.

Type IVD waxy bitumens

Representative chromatograms for Type IVD waxy bitumens are shown in Figure 121. Preliminary assessment of the biomarker compounds identified by TIC GC-MS, SIM GC-MS and MRM GC-MS-MS for the least altered specimens (summarised in Table 35) suggest they are derived from a marine carbonate with marine algal and little or no higher plant input. However, the presence of high-molecular-weight *n*-alkanes may also indicate terrestrial input from higher plants, despite no other biomarkers supporting this.

The absence of botryococcane, oleanane and bicadinanes precludes an Indonesian origin.

Table 35: Summary of source characteristics and key features of Type IVD waxy bitumens.

| Oil Family | Source Characteristics | Key Features |
|-----------------------|---|--|
| Type IVD waxy bitumen | Marine carbonate with marine algal & little or no higher plant input. | Pr/Ph absent (biodegradation) |
| | | Botryococcane absent |
| | | C_{27}/C_{29} sterane <1 (possible artefact of heavy biodegradation) |
| | | 24- <i>n</i> -propylcholestane (high) |
| | Presence of high molecular weight <i>n</i> -alkanes may also indicate terrestrial input from higher plants, although no other biomarkers support this | Dinosterane (low) |
| | | C_{27} dia/(dia+reg) sterane = 0.19 |
| | | C_{30} 4-Me sterane < C_{29} sterane |
| | | C_{26}/C_{25} tricyclic terpane = 0.76 |
| | Origin unknown | C_{29}/C_{30} $\alpha\beta$ hopane = 1.36 |
| | | C_{35}/C_{34} homohopane = 0.96 |
| | | C_{35} homohopane index = 0.08 |
| | | 29,30-bisnorhopane |
| | | Gammacerane |
| | | Oleanane absent |
| | | Bicadinanes absent |
| | | TPP (moderate) |

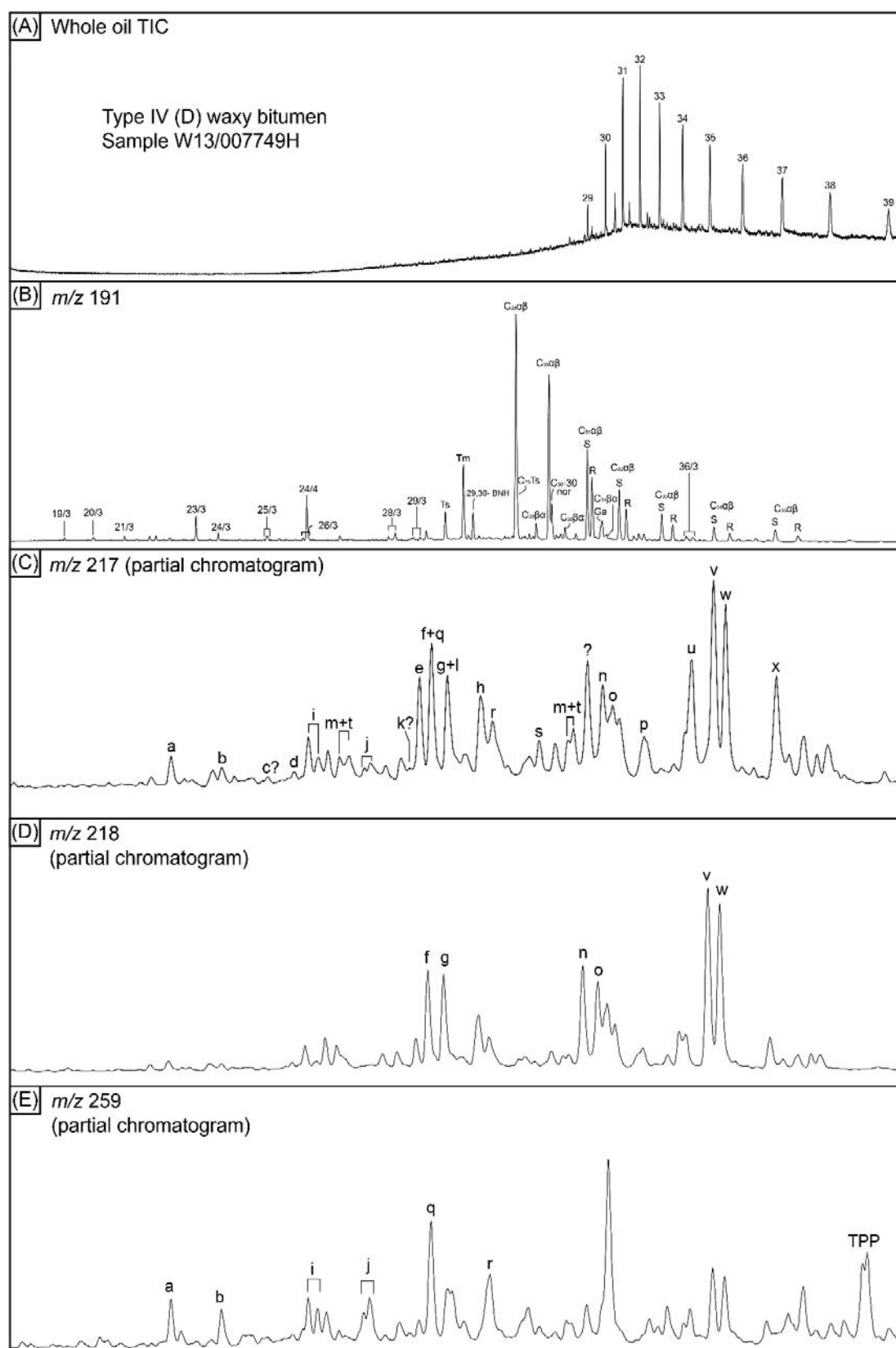


Figure 121: Representative chromatograms for Type IVD waxy bitumen. (A) Whole-oil GC-MS TIC showing alkane distribution. (B) m/z 191 chromatogram showing distribution of terpanes. (C) m/z 217 chromatogram showing distribution of steranes and diasteranes. (D) m/z 218 chromatogram showing distribution of C27-C29 $\alpha\beta$ steranes. (E) m/z 259 chromatogram showing distribution of C27-C29 $\beta\alpha$ diasteranes and TPP. For peak identifications refer to tables 18 and 19.

Type IVE waxy bitumens

Representative chromatograms for Type IVE waxy bitumens are shown in Figure 122. Preliminary assessment of the biomarker compounds identified by TIC GC-MS and SIM GC-MS for the key specimen (summarised in Table 36) suggests it is derived from a marine carbonate source deposited in a hypersaline environment with minor terrestrial organic matter input.

The presence of oleanane could suggest an Indonesian origin, although this requires confirmation by GC-MS-MS of the presence/absence of bicadinane, and further interpretation of 24-*n*-propylcholestane to confirm its marine source affinity, which is in progress. As such, this bitumen is currently of unknown origin.

Table 36: Summary of source characteristics and key features of Type IVE waxy bitumens.

| Oil Family | Source Characteristics | Key Features |
|-----------------------|--|---|
| Type IVE waxy bitumen | Marine carbonate source deposited in a hypersaline environment with minor terrestrial organic matter input. | Pr/Ph absent (biodegradation) |
| | | Botryococcane absent |
| | | C_{27}/C_{29} sterane >1 |
| | Further interpretation requires confirmation of presence/absence of 24- <i>n</i> -propylcholestane and bicadinane. | 24- <i>n</i> -propylcholestane (TBD) |
| | | C_{30} 4-Me sterane < C_{29} sterane |
| | | C_{27} dia/(dia+reg) sterane = 0.36 |
| | | C_{26}/C_{25} tricyclic terpane = 0.63 |
| | Origin unknown | C_{24} tetracyclic/ C_{23} tricyclic terpane ≥1 |
| | | C_{29}/C_{30} αβ hopane = 1.10 |
| | | C_{35}/C_{34} homohopane = 1.07 |
| | | C_{35} homohopane index = 0.10 |
| | | Gammacerane |
| | | Oleanane (low) |
| | | Bicadinanes (TBD) |
| | | TPP (low) |

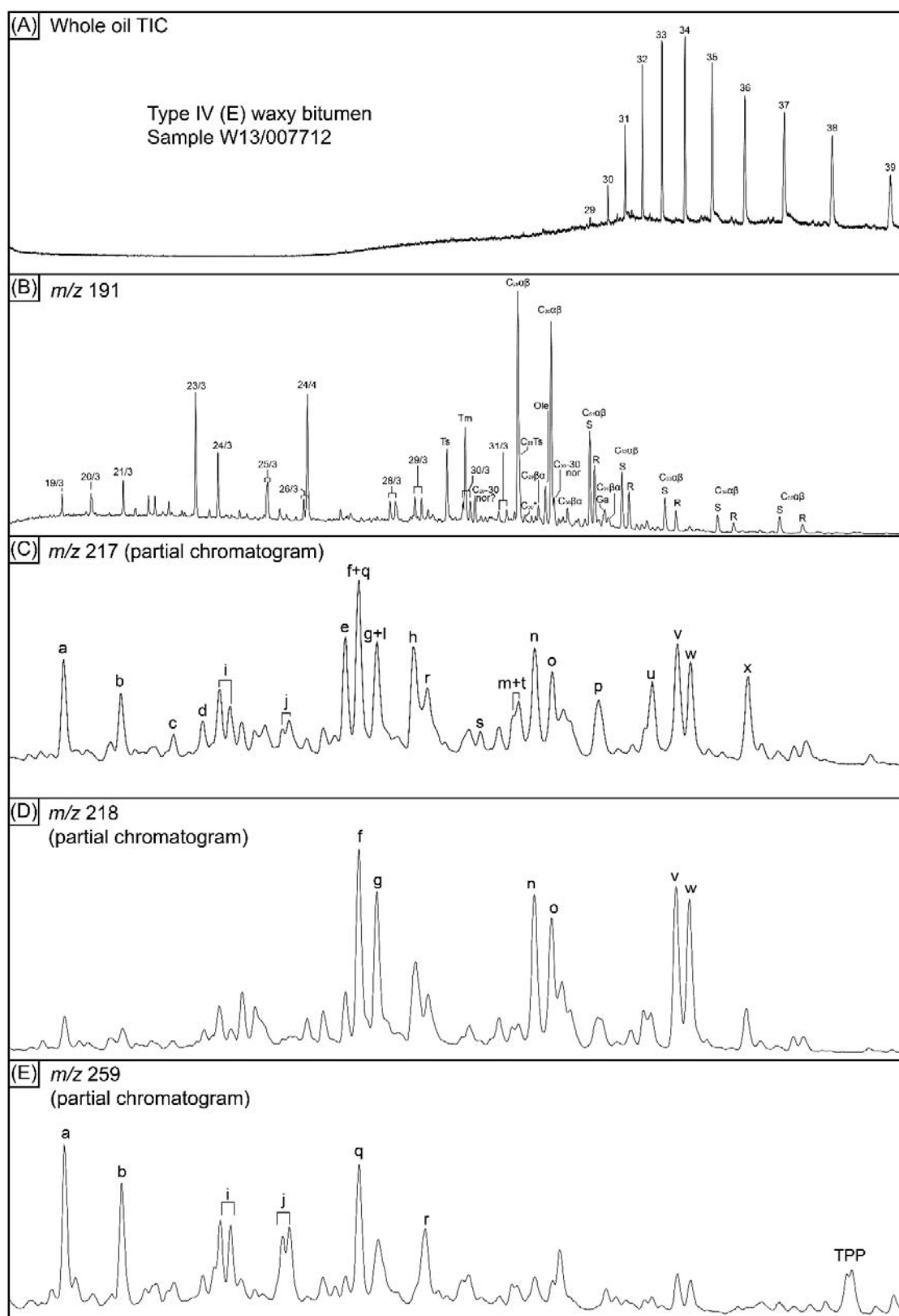


Figure 122: Representative chromatograms for Type IVE waxy bitumen. (A) Whole-oil GC-MS TIC showing alkane distribution. (B) m/z 191 chromatogram showing distribution of terpanes. (C) m/z 217 chromatogram showing distribution of steranes and diasteranes. (D) m/z 218 chromatogram showing distribution of C27-C29 $\alpha\beta$ steranes. (E) m/z 259 chromatogram showing distribution of C27-C29 $\beta\alpha$ diasteranes and TPP. For peak identifications refer to tables 18 and 19.

Sandy River soft bitumens

Representative chromatograms for the Sandy River soft bitumen are shown in Figure 123.

Preliminary assessment of the biomarker compounds identified by TIC GC-MS, SIM GC-MS and MRM GC-MS-MS for the key specimens (summarised in Table 37) suggest them to be derived from a deltaic shale deposited under sub-oxic conditions with terrestrial organic matter input (or having migrated through a deltaic sequence).

The presence of oleanane, bicadinanes and bisnorlupanes is consistent with a Cenozoic Indonesian origin, potentially in the offshore Kutei Basin.

Table 37: Summary of source characteristics and key features of Sandy River soft bitumens.

| Oil Family | Source Characteristics | Key Features |
|--------------------------|---|---|
| Sandy River soft bitumen | Cenozoic deltaic shale deposited in suboxic conditions with terrestrial organic matter input (or migrated through a Cenozoic delta) | Pr/Ph = 1.0-1.1 (potentially minor alteration) |
| | | Botryococcane absent |
| | | C ₂₇ /C ₂₉ sterane >1 |
| | | 24- <i>n</i> -propylcholestane (low) |
| | Presence of oleanane, bicadinanes & bisnorlupanes is consistent with an Indonesian origin. Potentially the offshore Kutei Basin (Curiale et al., 2005, 2006), or the Misool seafloor seep (Noble et al., 2009). | C ₃₀ 4-Me sterane < C ₂₉ sterane |
| | | C ₂₇ dia/(dia+reg) sterane = 0.35 |
| | | C ₂₆ /C ₂₅ tricyclic terpane = 1.08 |
| | | C ₂₉ /C ₃₀ αβ hopane = 0.61 |
| | | C ₃₅ /C ₃₄ homohopane = 0.75 |
| | | C ₃₅ homohopane index = 0.05 |
| | | Gammacerane |
| | | Oleanane (high) |
| | | Bicadinanes (high) |
| | | TPP (moderate) |
| | | Bisnorlupanes, bisnoroleanane & taraxastane |

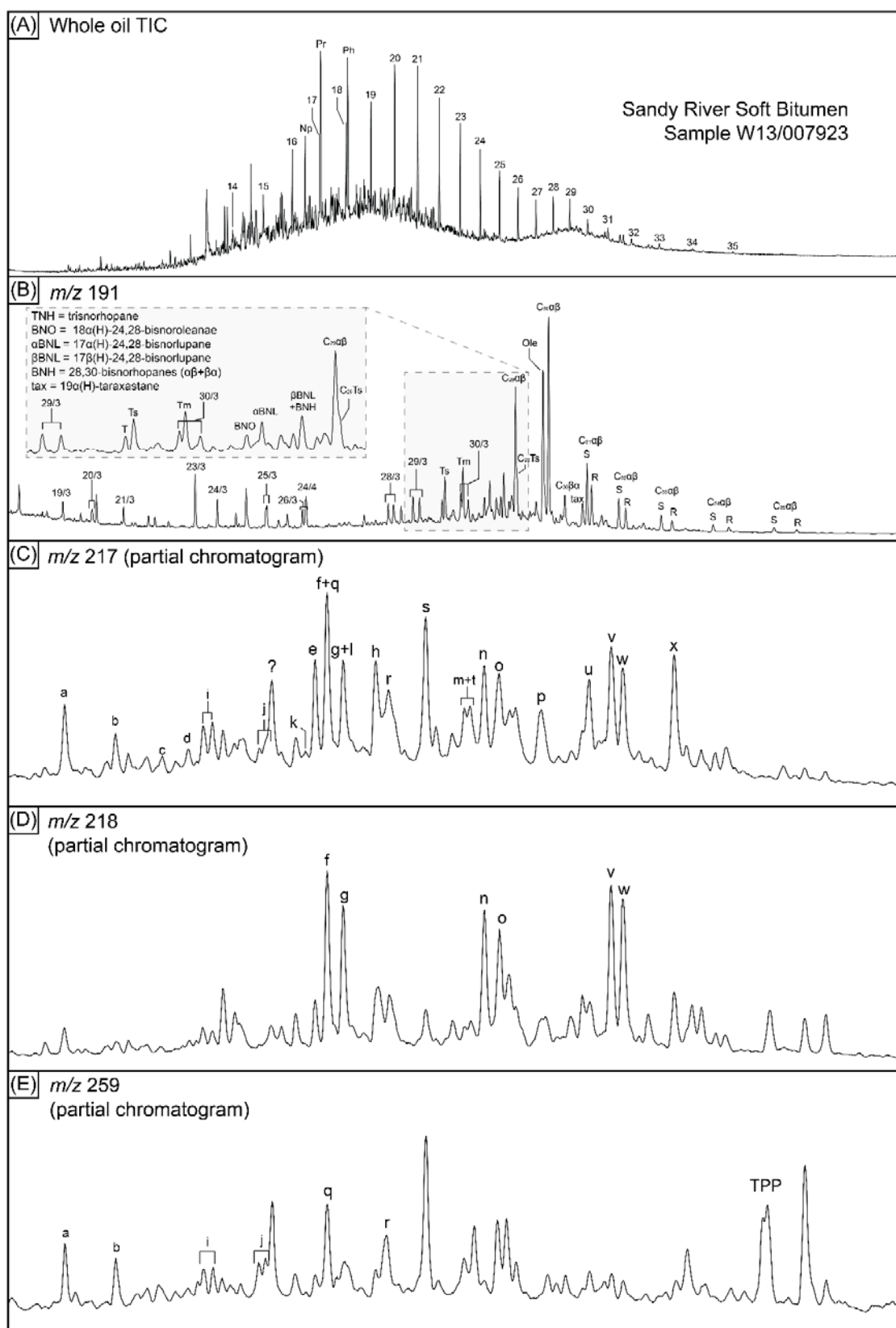


Figure 123: Representative chromatograms for Sandy River soft bitumen. (A) Whole-oil GC-MS TIC showing alkane distribution. (B) m/z 191 chromatogram showing distribution of terpanes. (C) m/z 217 chromatogram showing distribution of steranes and diasteranes. (D) m/z 218 chromatogram showing distribution of C27-C29 $\alpha\beta$ steranes. (E) m/z 259 chromatogram showing distribution of C27-C29 $\beta\alpha$ diasteranes and TPP. For peak identifications refer to tables 18 and 19.

Comparison with Statistical Data Treatment (HCA)

Comparison of the individual biomarker classifications of coastal bitumen samples compared to hierarchical cluster analysis based on specific compound ratios is shown in Figure 124. Overall there is a strong agreement between the individually assessed families and cluster distribution, with many sub-groups corresponding to the individually identified families. Minor exceptions occur where samples interpreted as belonging to the same oil family are placed in different clusters. These exceptions include families with a low number of samples (e.g. Type IIIC), samples which have undergone biodegradation (e.g. degraded asphaltites) and samples with poor quality biomarker response (Type IVA). Additionally, some samples identified as different families were not included in the sample suite used for HCA, These include:

- The single sample (W13/007503) which defines the Type IIIE oil family and requires reanalysis for higher quality data before statistical treatment.
- The single sample (W13/007857A) which defines the Type IVC oil family and did not have compound ratios available during HCA sample selection.
- The samples classified as Type IVD, as the freshest examples of this family, have undergone significant biomarker degradation and should therefore not be included for correlative purposes.

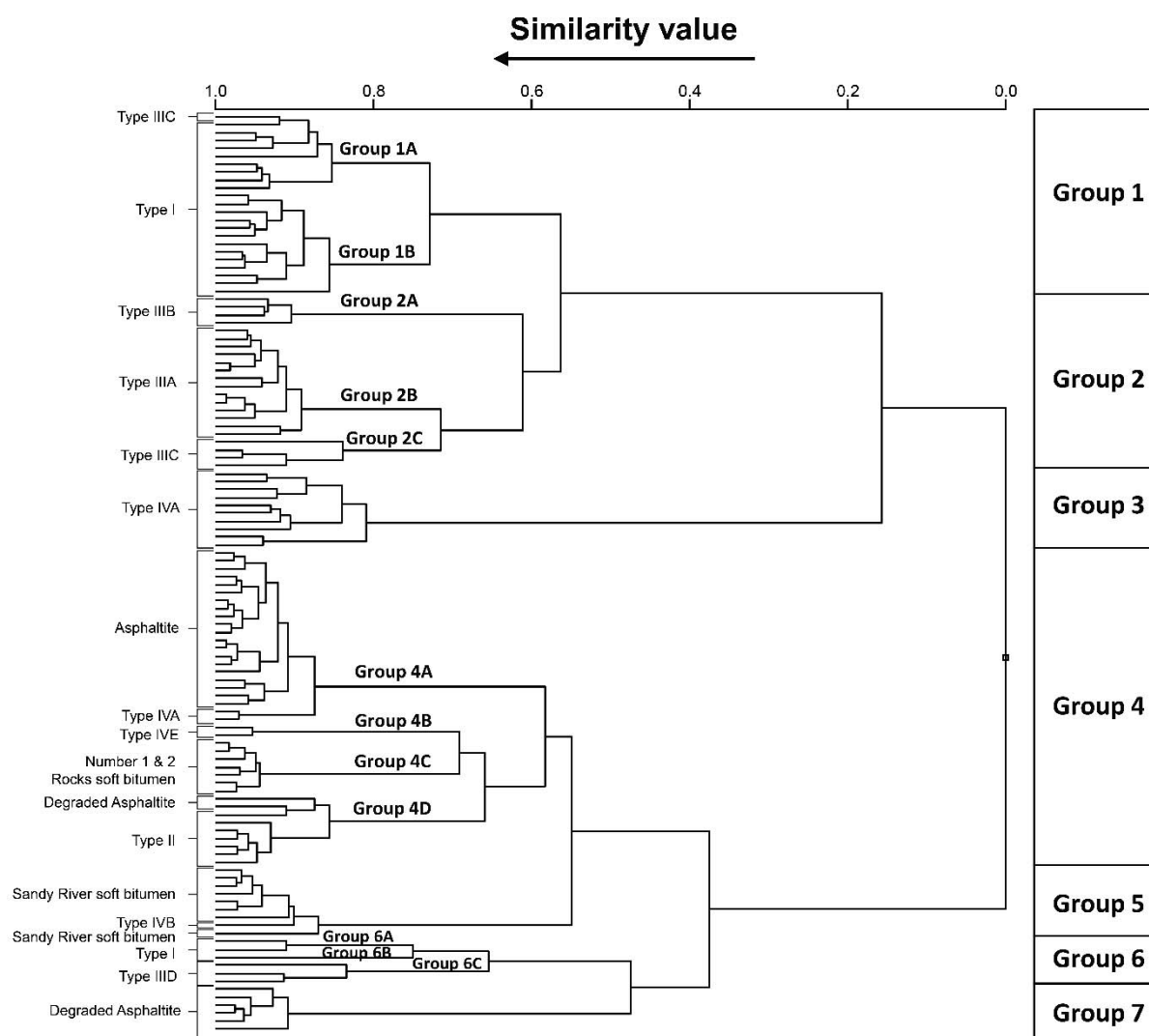


Figure 124: Hierarchical cluster analysis (HCA) of coastal bitumen samples. Left labels correspond to individual oil family assessment.

Comparison with other data sets

McKirdy et al., (1986) reported the discovery of botryococcane in a suite of waxy coastal bitumens collected during 1983 from ocean beaches in southeastern South Australia and western Victoria. This rare acyclic isoprenoid biomarker, derived from the freshwater chlorophyte alga *Botryococcus braunii*, had hitherto been found *only* in Cenozoic lacustrine oils and source rocks from Central Sumatra (Seifert & Moldowan, 1981) and an Eocene oil shale from China (Brassell et al., 1986). It was some years before subsequent workers realised the potential significance of these respective findings and concluded that the stranded bitumens had most likely originated from one or more basins in South East Asia (Currie et al., 1992; Padley et al., 1993; McKirdy et al., 1994; McGowran et al., 1997).

A follow-up study of 111 individual specimens of such bitumen collected from the same coastline between 1961 and 1992 (Padley, 1995; Edwards et al., 2016) showed them to be variously weathered high-wax crude oils of paraffinic to aromatic-intermediate bulk composition. Elemental,

isotopic and biomarker differences allowed their assignment to at least five geochemically distinct oil families. The key distinguishing features of these families, and their comparison with Indonesian oil families, are elaborated in Edwards et al., (2017), from which the following summary is taken.

Waxy bitumen (tar ball) geochemistry: a 1995 perspective

The five aforementioned bitumen families are summarised in Table 38. Their inferred source facies range from deep freshwater lacustrine through paludal and deltaic to euxinic marine, more than likely deposited within different sedimentary basins. Family 1, 2 and 3 bitumens all contain biomarkers derived from the freshwater alga *Botryococcus* sp. and tropical angiosperms (notably dipterocarps). Similar biomarker assemblages are unknown in Australian sedimentary basins but are common in Cenozoic crude oils and source rocks throughout Southeast Asia. Family 4 bitumens lack these biomarkers but do contain dinosterane and 24-*n*-propylcholestane, indicative of a marine source affinity, while the carbon-isotopic signatures and high pristane/phytane ratios of Family 5 bitumens are consistent with their origin from coal-rich source rocks deposited in fluvial to deltaic sedimentary successions.

The prominence of bicadinanes in the ostensibly Cenozoic biomarker signatures of the southern Australian waxy coastal bitumen Families 1–3 (Table 38) appears to preclude their local origin. Bicadinanes are derived principally from tropical angiosperms of the family *Dipterocarpaceae*, trees that first appeared in the Oligocene and now dominate the lowland rain forests of Southeast Asia, but do not grow in Australia (Paijmans et al., 1976; Ashton, 1982; Ghazoul, 2016). Fossil evidence suggests that they originated in Africa, and subsequently migrated via India to Asia. However, no dipterocarp micro- or megafossils have been identified in Cenozoic sediments anywhere in Australia (Hill, 1994). Therefore, it seems reasonable to conclude that these waxy bitumens do not originate from Australian sedimentary basins. The trace levels of bicadinanes (\pm oleanane) found in a Jurassic crude oil and source rock from the Eromanga Basin (Armanios et al., 1995) and Late Cretaceous-sourced oils in the Gippsland Basin (George et al., 1998; Volk et al., 2010) are attributable to a more general angiosperm flora (van Aarssen et al., 1994; Murray et al., 1994b). The reported occurrence of these biomarkers in oils from the Perth Basin (Summons et al., 1995) is now attributed to laboratory contamination (D.S. Edwards, pers. comm., 2017). An Australian origin for the Family 4 and 5 waxy bitumens remains a possibility, with further studies of potential source rocks and generated hydrocarbons within the Otway, Bight, Bremer and offshore Perth basins being required for definitive oil-source and oil-oil correlations.

Table 38: Diagnostic characteristics and source affinity of waxy bitumens collected from ocean beaches in South Australia and western Victoria prior to 1995 (after Edwards et al., 2017).

| FAMILY | S WT % | Pr/Ph | BI | BOT/N-C29 | STERANES | 24-N-PROPYL | DINO |
|-------------|---------|---------|---------|-----------|-------------------|-------------|--------|
| 1 n = 35 | <0.3 | 0.2–2.6 | 530–870 | 0.16–0.86 | 29 > 27 > 28 | A | A |
| 2 n = 16 | 0.6–2 | 0.7–1.7 | nd | 0.15–0.71 | 29 \geq 27 > 28 | P | P |
| 3 n = 33 | 1.1–2.6 | 0.5–1.1 | 104–173 | 0.04–0.14 | 27 > 29 > 28 | P or A | P or A |
| 4 | 0.9 | 0.5–1.4 | 0 | 0 | 27 > 29 > 28 | P | P |

| | | | | | | | |
|-------|-----|------|----|----|----|----|----|
| n = 7 | | | | | | | |
| 5 | 0.2 | 4–11 | nd | nd | nd | nd | nd |
| n = 5 | | | | | | | |

| | HOP/STER | OLEANANE | BICADINANES | CV* | SOURCE AFFINITY |
|---|----------|----------|-------------|-------|--|
| 1 | 1.7–4.5 | P | P | <0.47 | Lacustrine shale Anoxic–suboxic Cenozoic |
| 2 | 1.1–6.7 | P | P | <0.47 | Lacustrine shale > marine carbonate Anoxic–suboxic Cenozoic |
| 3 | 0.6–1.3 | P | P | <0.47 | Marine carbonate > lacustrine shale Anoxic/euxinic Cenozoic |
| 4 | 0.8–1.8 | A | A | <0.47 | Marine carbonate or calcareous shale Anoxic–suboxic Mesozoic |
| 5 | nd | nd | nd | >0.47 | Non-marine (?) coal Oxic |

* $CV = -2.53 \text{ }^{13}C_{\text{sat}} + 2.22 \text{ }^{13}C_{\text{aro}} - 11.65$ (Sofer, 1984)

P = present A = absent nd = not determined

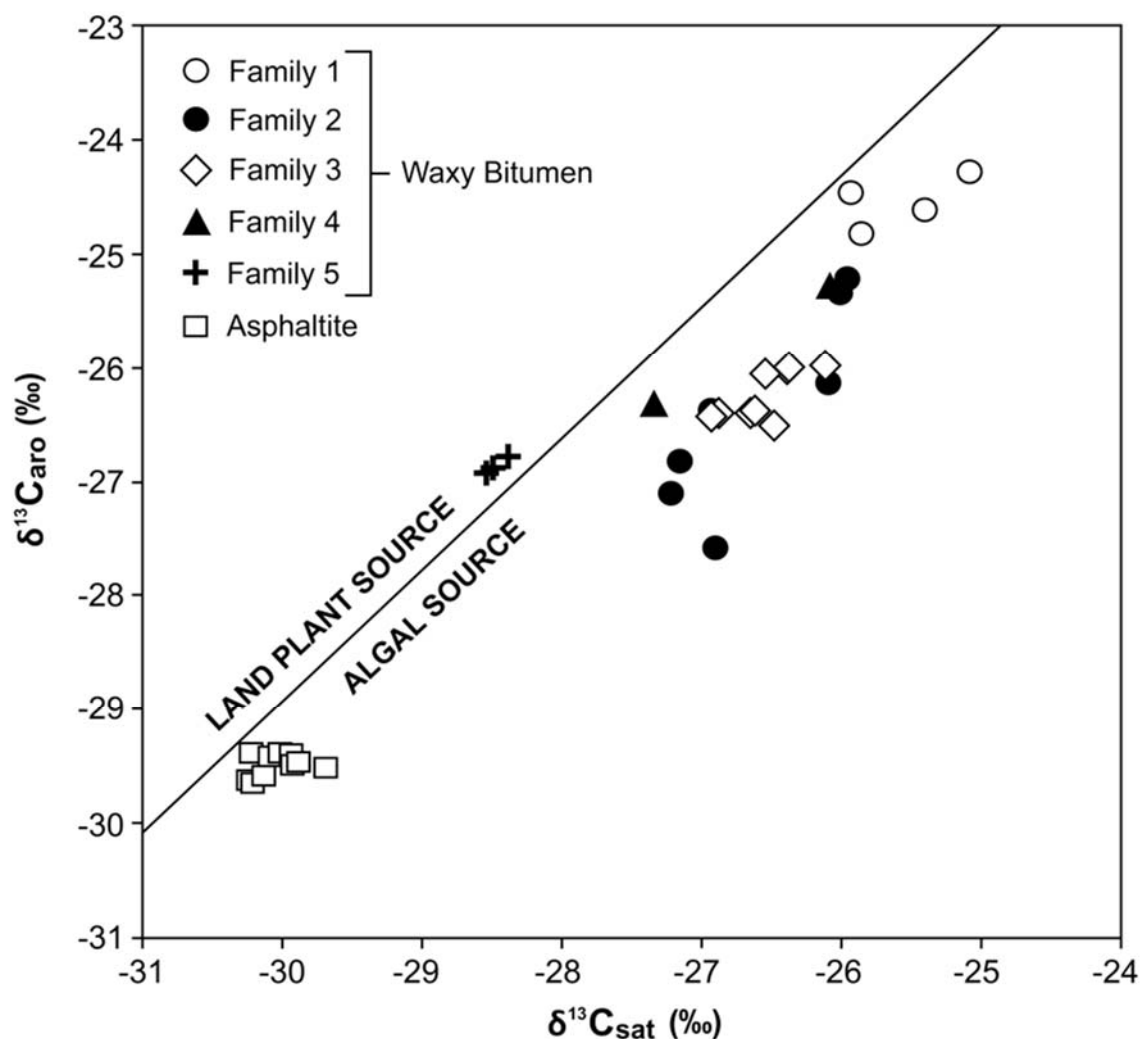


Figure 125: Carbon isotope signatures of coastal bitumens collected from southern Australian beaches prior to 1995 (after Edwards et al., 2016).

Comparison with Indonesian oil families

The high concentrations of bicadinane found in the Family 1, 2 and 3 bitumens are in fact typical of Cenozoic oils and source rocks from Indonesia (Cox et al., 1986; Teerman et al., 1987; van Aarssen et al., 1992; Sosrowidjojo et al., 1994) and Papua New Guinea (Murray et al., 1993; Waples & Wulff, 1996). They reflect the predominance of dipterocarps in the Cenozoic flora of this region. Given that the biomarker signatures of the complete range of waxy bitumens indicate their derivation from lacustrine through marginal marine to paludal (coal-bearing) organic facies (Table 38), it is informative to note similar signatures and source affinities in oils from Indonesia (Table 39; Figure 126 to Figure 129).

Table 39: Key biomarker characteristics of West Indonesian oil families, their locations and their likely source affinities (after Edwards et al., 2017).

| FAMILY | KEY BIOMARKER SIGNATURES | BASINS | SOURCE LITHOFACIES & AGE | DATA SOURCES |
|------------------------------|---|---|--------------------------------------|---------------|
| Fresh/deep lacustrine | Botryococcane C ₃₀ Tetracyclic polyprenoid (TPP)* C ₃₀ 4-methylsteranes C ₂₆ /C ₂₅ tricyclic terpane >>1 Ts/Tm >1 Oleanane Bicadinanes Hopanes > Steranes Pristane/phytane = 1.5–3 24- <i>n</i> -Propylcholestane absent | Central Sumatra South Sumatra Sunda | Shale Cenozoic | 1, 2, 3, 4, 7 |
| Brackish lacustrine | As above, but with minor or no botryococcane & higher abundances of terrigenous triterpanes (oleanane, bicadinanes) Gammacerane present | Central Sumatra South Sumatra Ombilin East Java | Shale Cenozoic | 1, 2, 3, 4, 7 |
| Terrigenous (fluvio-deltaic) | C ₂₉ sterane dominant Bicadinanes Oleanane C ₂₆ /C ₂₅ tricyclic terpane <1 Pristane/phytane >3 | North Sumatra Central Sumatra South Sumatra West Nantuna Northwest Java | Coal, carbonaceous shale Cenozoic | 2, 3, 4, 5 |
| Marine | C ₂₇ sterane dominant 24- <i>n</i> -Propylcholestane present C ₂₉ /C ₃₀ hopane >1 Pristane/phytane = 1–2.5 | North Sumatra East Nantuna | arbonate Cenozoic | 2, 3, 4, 6 |

* Reported as unknown 'lacustrine classifier' by ten Haven & Schiefelbein (1995); subsequently identified by Holba et al., (2000)

Key to data sources:

1. Seifert & Moldowan (1981)
2. Robinson (1987)
3. ten Haven & Schiefelbein (1995)
4. Schiefelbein & Cameron (1997)
5. van Aarssen et al., (1992)
6. Subroto et al., (1992)
7. Hwang et al., (2002)

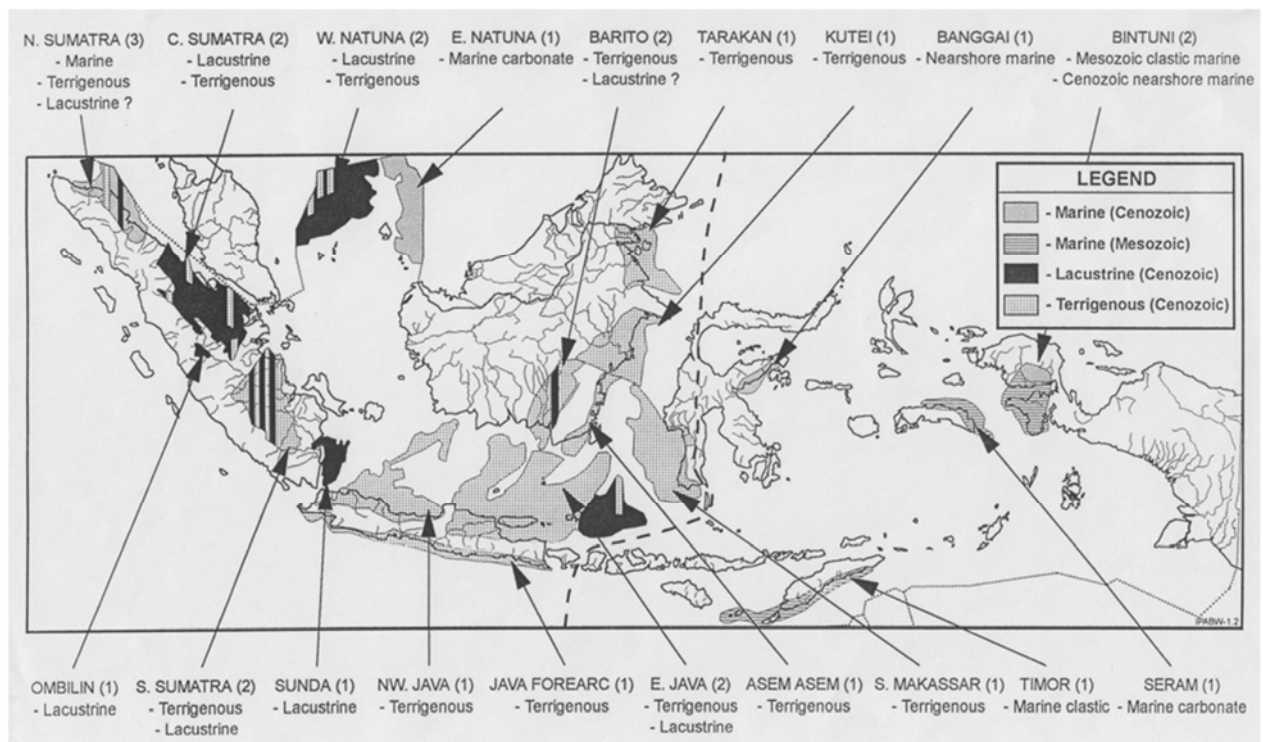


Figure 126: Map showing the location of the Indonesian basins sampled and the geographical distribution of their different oil types (after ten Haven & Schiefelbein, 1995).

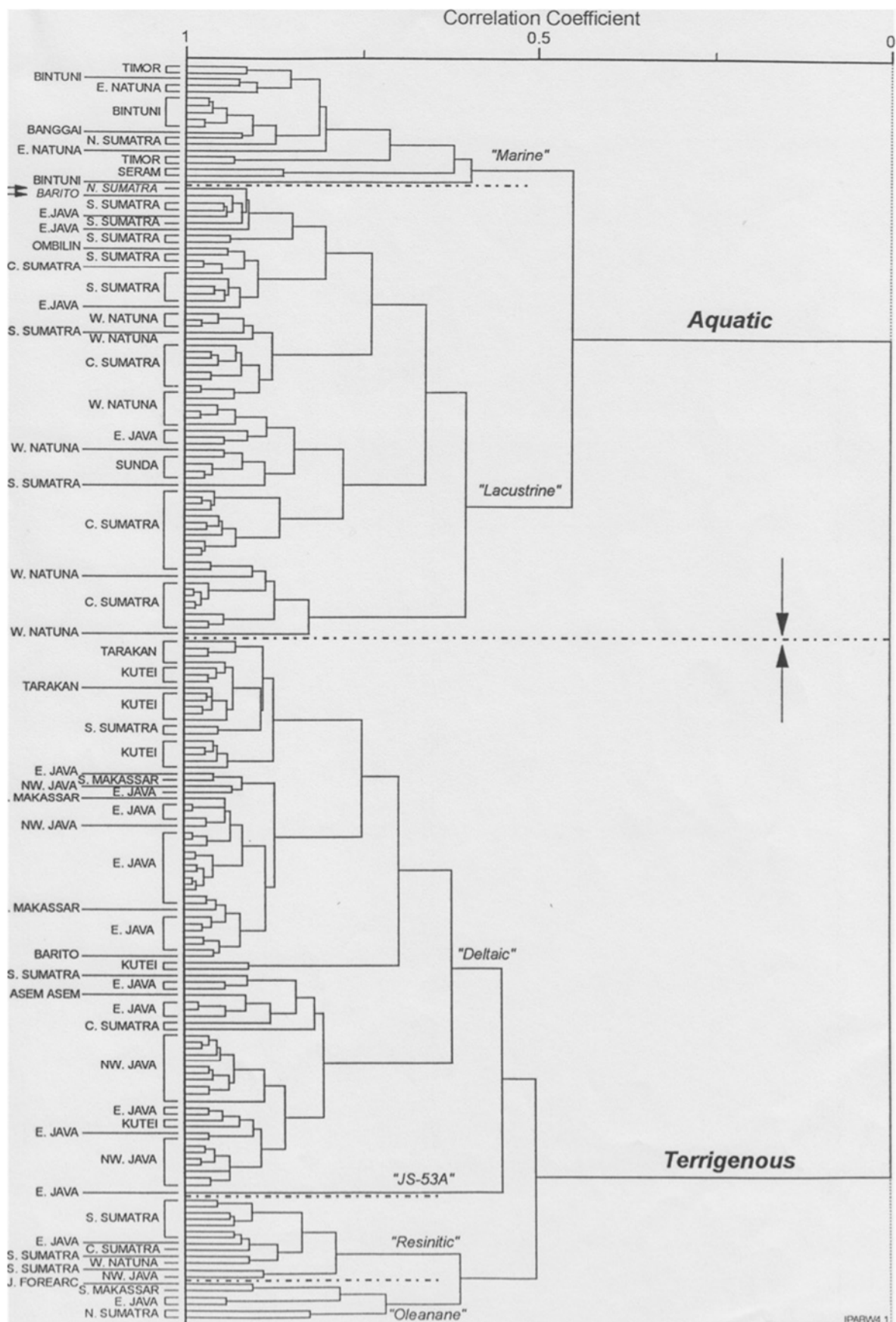


Figure 127: Dendrogram showing hierarchical clustering of 193 oils from 19 Indonesian sedimentary basins (after ten Haven & Schiefelbein, 1995).

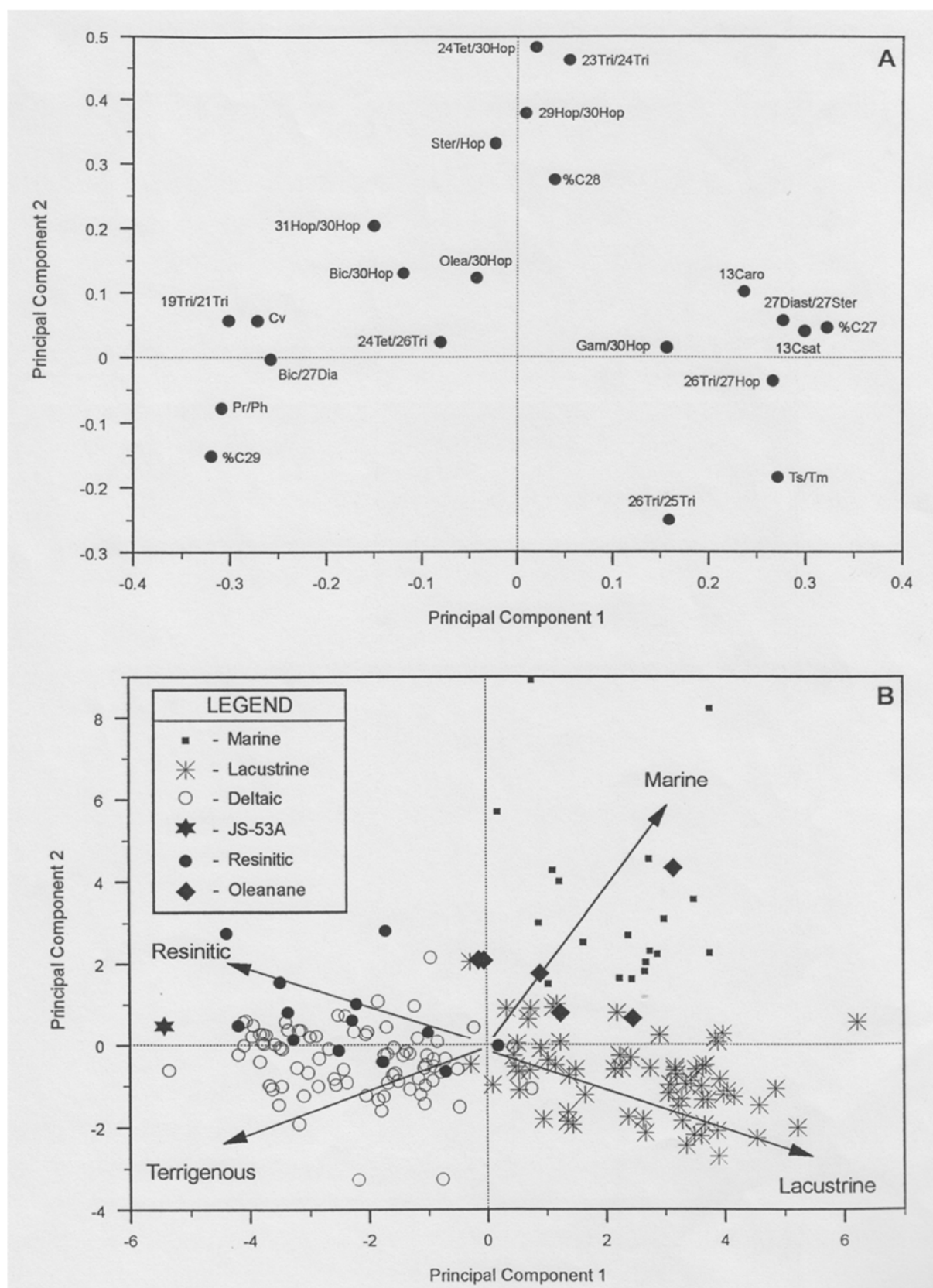


Figure 128: Principal components analysis (PCA) of geochemical data on Indonesian oils (after ten Haven & Schiefelbein, 1995). The key discriminators are shown in panel A.

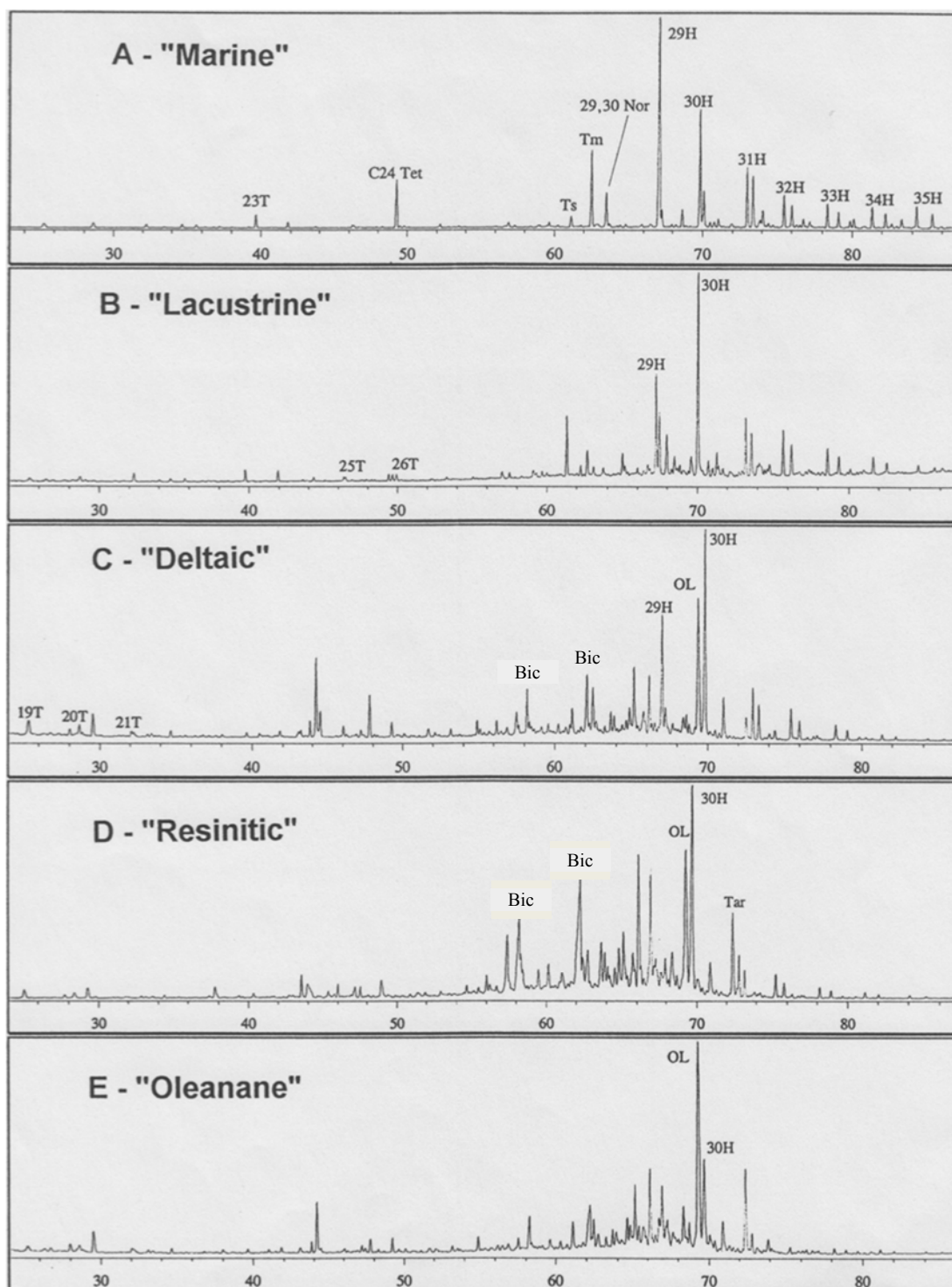


Figure 129: Partial m/z 191 chromatograms of five representative Indonesian oil types (after ten Haven and Schiefelbein, 1995).

T = tricyclic terpene
Tet = tetracyclic terpene
H = hopane
Bic = bicadinane
OL = oleanane
Tar = taraxerane

Waxy oils of lacustrine source affinity are confined to basins located in western Indonesia (Figure 126). Arguably the best documented are those in the onshore Central and South Sumatra basins and the offshore Sunda and East Java basins (Schiefelbein & Cameron, 1997; Hwang et al., 2002). Their respective source rocks, viz. the Brown Shale Formation, Pematang Group (Williams et al., 1985) and the Banuwati Shale (Robinson, 1987), are of Eocene to Oligocene age. Lacustrine oils likewise occur further north in the offshore East Nantuna, West Natuna and Anambas basins (Noble et al., 2009).

Seifert & Moldowan (1981) were the first to report that lacustrine oils produced from the Central Sumatra Basin have divergent geochemical signatures. The biomarker assemblage of the heavily biodegraded Duri-1 crude oil matches that of the Minas-1 oil, both containing abundant botryococcane. In other oils, such as the South Bekasap-1 crude, the concentration of botryococcane is much lower; and in the Pematang-1 oil this freshwater algal marker is entirely absent, a more saline lacustrine setting for its source rock being indicated by the presence of gammacerane (Table 39). With access to larger datasets, subsequent workers have divided the Indonesian lacustrine oil family into subgroups: Type A, B & C (Figure 130: ten Haven & Schiefelbein, 1995) and Groups I–V (Hwang et al., 2002). Across Sumatra this compositional heterogeneity has been attributed to differences in water chemistry in different sub-basins (Katz & Mertani, 1989) or, alternatively, variation of the Brown Shale source rock facies within a single deep lake system (Schiefelbein & Cameron, 1997).

The biomarker assemblages of the southern Australian waxy bitumens (especially Families 1–3) show many similarities to some of the lacustrine West Indonesian oils (Table 39), but an exact match is not evident. For example, the deep lacustrine Minas-1 oil from the Central Sumatra Basin is a high wax, low sulphur, paraffinic crude oil that closely resembles the Family 1 bitumens. Its biomarker signatures include unusually high concentrations of botryococcane, C₃₀ 4-methylsteranes, bicadinane and methylbicadinane; a ethylcholestane-dominant sterane distribution; the presence of oleanane; and an absence of C₃₀ 24-*n*-propylcholestane and dinosterane (Seifert & Moldowan, 1981; Currie et al., 1992; Summons et al., 1993; McKirdy et al., 1994; Moldowan et al., 2005), all features of the Family 1 bitumens (Table 38). Moreover, its C-isotopic signatures ($\delta^{13}\text{C}_{\text{sat}} = -26.2\text{‰}$, $\delta^{13}\text{C}_{\text{aro}} = -24.7\text{‰}$, CV = -0.17: Peters et al., 2005) also plot close to those of the least weathered Family 1 bitumens (Figure 125). However, its bicadinane distribution differs significantly from that of a typical Family 1 bitumen (Edwards et al., 2017, Figure 125), preventing their exact correlation.

Other Indonesian waxy crude oils originated from coal-rich fluvial deltaic sediments of Oligocene-Miocene age and are assigned to the terrigenous family (Table 39). Source rocks in this category include the coals of the Sihapas Group, Central Sumatra Basin and the coals and shales of the Talang Akar Formation in the South Sumatra Basin, the Sunda Basin and the Ardjuna Sub-basin (Robinson, 1987; Pramono et al., 1990; Noble et al., 1991). It is worth noting that the terrigenous oil family of ten Haven & Schiefelbein (1995) is subdivided into a major deltaic sub-group and two minor sub-groups, resinitic and oleanane-rich (Figure 127 and Figure 128), according to their relative abundances of bicadinanes and oleanane (Figure 129).

The Australian waxy bitumens of Family 5 (Table 38) are insufficiently characterised to ascertain the degree to which they resemble the terrigenous oils of western Indonesia and might therefore be of local (intra-Bight Basin) origin.

With the exception of several examples from the North Sumatra and East Nantuna basins, most Indonesian crude oils of marine origin are located in the eastern half of the archipelago (ten Haven & Schiefelbein, 1995; Peters et al., 1999; Noble et al., 2009). Here their source rocks may be of either Cenozoic or Mesozoic age and include both carbonate and shale lithofacies, whereas in western Indonesia oil-prone marine source rocks are both less common and all of Cenozoic age (Price et al., 1987; Robinson, 1987). It is in Eastern Indonesia that most of the known offshore oil seeps occur (Figure 130). Those located in Seram and the Timor Sea are of marine source affinity and thought to have originated in Mesozoic carbonate and shale lithofacies (Price et al., 1987; Noble et al., 2009). In this respect, they appear similar to the Family 4 waxy bitumens which notably lack oleanane and bicadinanes (Table 38).

An alternative origin for the marine waxy bitumens of Family 4 is from the Australian North West Shelf and Perth basins where marine oils are known (Edwards & Zumberge, 2005 and references therein). In contrast to Southeast Asia, the passive margin of Australia has few documented seepage sites. Where detected, seepage appears to be predominantly gas rather than oil (Logan et al., 2010). However, in the Browse Basin on the Yampi Shelf (in the vicinity of the Cornea field) natural oil and gas seeps have been sampled (Rollet et al., 2006; Burns et al., 2010), and a microseep of oil was also found at one site in the southern Bonaparte Basin (Stalvies et al., 2017; Figure 131). These seeps were correlated with crude oils (Cornea and Gwydion) from the Yampi Shelf and determined to be sourced by the Early Cretaceous Echuca Shoals Formation (Logan et al., 2008; Stalvies et al., 2017). However, the C-isotopic compositions of these oils and source rocks are lighter than those displayed by the Family 4 waxy bitumens (Figure 125), ruling out the Browse Basin as their potential source. Likewise, the Early Triassic-sourced marine oils from the Perth Basin have significantly lighter isotopic compositions than the Family 4 waxy bitumens and contain a distinctive C₃₃ *n*-alkylcyclohexane (Summons et al., 1995; Thomas & Barber, 2004) not found in the bitumens, thereby precluding their correlation. The majority of Jurassic marine oils in the Northern Carnarvon and Bonaparte basins are non-waxy crudes sourced by organic-rich marine shales within the Dingo Claystone and Vulcan Formation (Edwards & Zumberge, 2005). However, since these basins also host some waxy Jurassic oils that are isotopically similar to the Family 4 waxy bitumens, further work is required to evaluate their possible common origin.

In summary, the southern Australian coastal waxy bitumens cannot yet be precisely correlated with any Southeast Asian oils. Nevertheless, the Family 1–3 waxy bitumens display sufficient similarities with oils from Indonesia and Papua New Guinea to be most likely derived from this region. An Australian origin for the Family 4 and 5 waxy bitumens remains a possibility, with further studies of potential source rocks and generated hydrocarbons within the basins along Australia's southern margin and North West Shelf being required for definitive oil-source and oil-oil correlations.

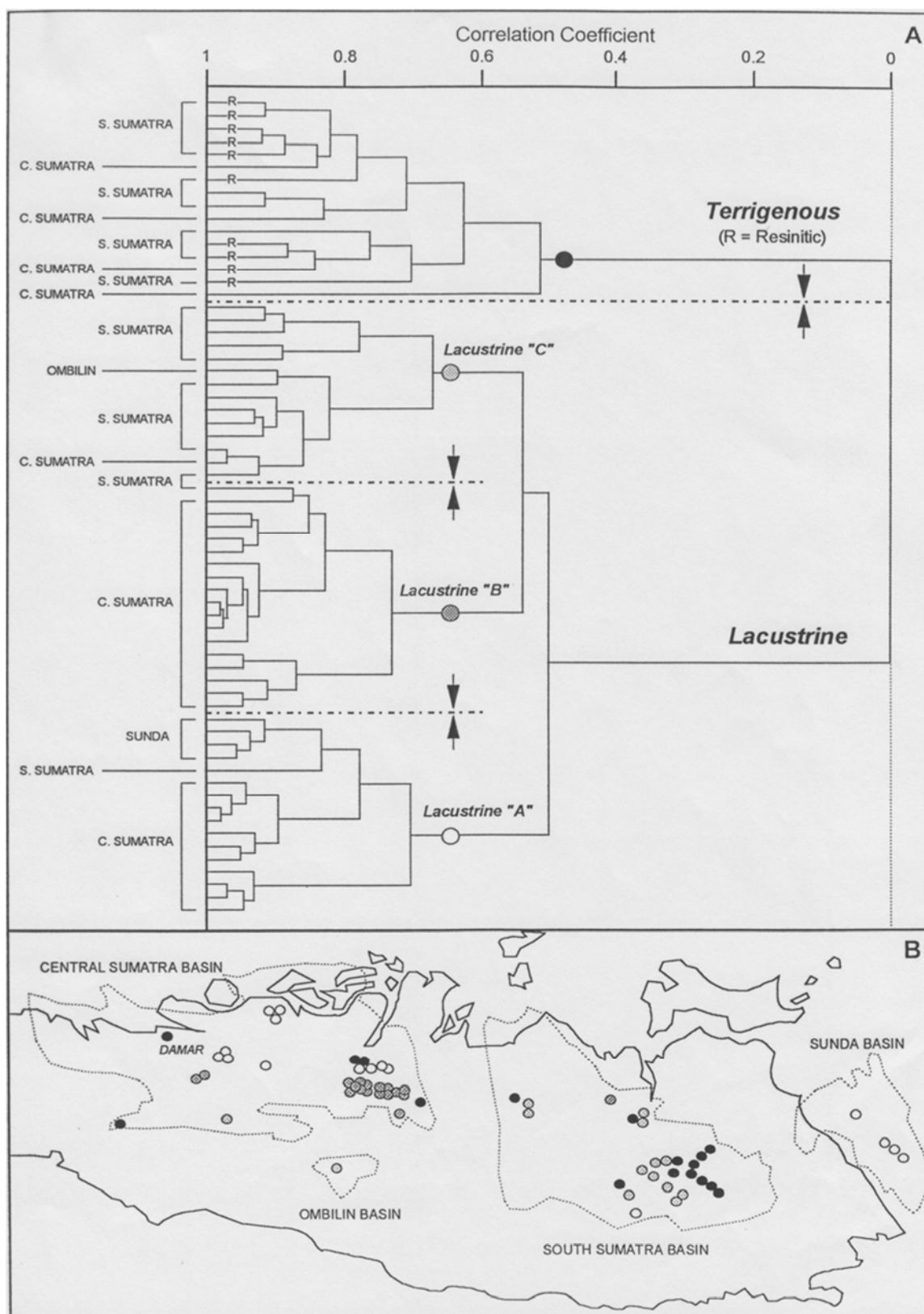


Figure 130: Dendrogram showing clustering of oils from Central and South Sumatra, and map illustrating the geographical distribution of different oil types (after ten Haven & Schiefelbein, 1995).

Possible modes of origin

Accepting that they are the remains of weathered Southeast Asian crude oils, the occurrence of these waxy bitumens in southern Australia has several possible explanations: jettisoned oil cargoes, tanker washings, leakage from oil pipelines, or natural ocean flotsam emanating from oil seeps.

Australia began importing crude oil during the mid-1950s and continues to import large quantities from Southeast Asia. The composition of many of these imported crudes is documented in a national oil-on-the-sea database (NOSID: Sandison & Edwards, 2001). Oil slicks from tanker washings and petroleum accidentally spilled from local shipping intermittently strand along the Victorian and South Australian coastline (Padley et al., 1993). The physical and chemical properties of these freshly spilled oils readily distinguish them from weathered waxy bitumen (Edwards et al., 2016). The latter is therefore thought not to be a by-product of local maritime activity in southern Australian waters. However, the Straits of Malacca and the Sunda Strait are major shipping routes where tanker cleaning operations are undertaken prior to reloading at Singapore (Figure 131). Regular oil spills in the western Java Sea since 2004 have been linked to both the high density of maritime traffic and leakage from submarine pipelines carrying oil from offshore production platforms (Putri et al., 2016).

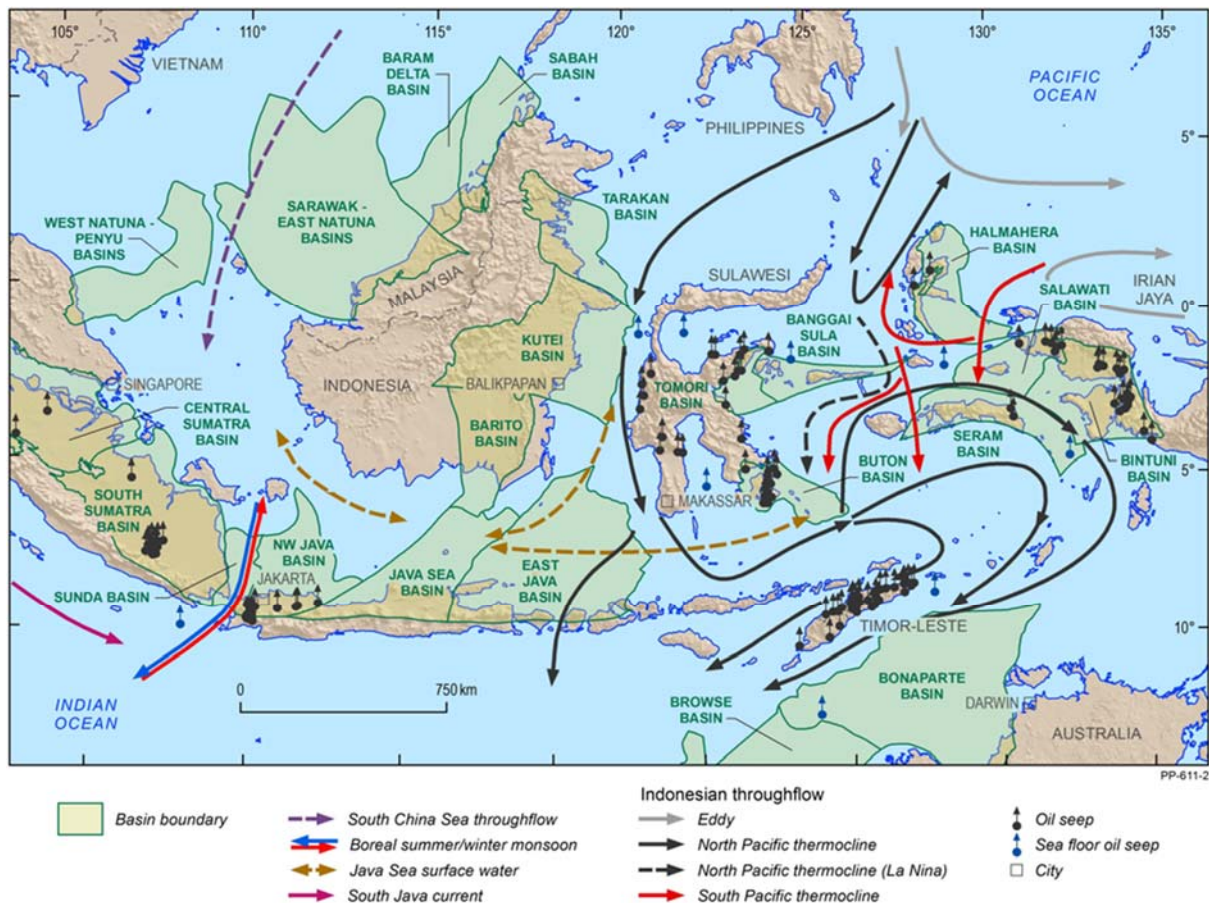


Figure 131: Map of selected sedimentary basins within the Indonesian Archipelago showing the locations of oil seeps and the pathways of the Indonesian and South China Sea throughflows (after Edwards et al., 2017 and references cited therein).

While active onshore oil seeps are common throughout the Indonesian Archipelago (Figure 131) and Papua-New Guinea (Livsey et al., 1992; Waples & Wulff, 1996), few overlie known oil fields and none of the giant fields are associated with seeps (Macgregor, 1995). In the case of the giant Minas Field,

the low ratio of gas to oil has reduced the capacity for vertical migration, making it difficult for the oil to escape to the surface. Unless adjacent to major rivers, the inland locations of these surface seeps make them unlikely sources for the Australian waxy bitumens.

Although fewer in number, more likely sources are submarine seeps such as those recently identified by multibeam echo sounder bathymetry and backscatter imaging in combination with deep-sea piston coring (Noble et al., 2009). As previously mentioned, the seeps located offshore from the islands of Timor and Seram (Figure 126) are potential points of origin for the marine Family 4 waxy bitumens. While no seeps have yet been identified in the offshore Sunda Basin (Macgregor, 1995), this Cenozoic lacustrine depocentre is the site of major lacustrine oil production and remains a possible source for the Family 1 bitumens. Likewise, the co-occurrence Cenozoic lacustrine and marine oils in the offshore East Natuna Basin (Noble et al., 2009) makes it a potential source for the mixed lacustrine/marine bitumens of Families 2 and 3 (Table 38). Natural seafloor seepage of crude oil into the ocean throughout the Indonesian Archipelago is now well established and would readily give rise to the seaborne waxy bitumens (tarballs) that ultimately strand in southern Australia. However, the fact that such seeps are generally episodic and ephemeral (Kvenvolden & Cooper, 2003) adds to the difficulty of linking a given bitumen stranding to its parent seep.

Potential GAB sources

The asphaltites are currently hypothesised to be derived from a Cretaceous source (Edwards et al., 1998; Hall et al., 2014), which is consistent with their potential origin in the Bight Basin. Additionally, the geochemistry of the soft bitumen collected from Number 1 & 2 Rocks in 2016 is similar to that of the asphaltites, indicating that they too may be of a local origin. These new soft bitumens have a different thermal maturity to the asphaltites, suggesting that their source may form the basis of a larger petroleum system in the GAB which in one region manifests itself as the well-studied asphaltite strandings, and in another as these soft bitumens.

Previous studies have linked most (although not all) families of waxy bitumen to sources in Indonesia (McKirdy et al., 1994; Currie et al., 1988; Edwards et al., 2016, 2017). However, the results of the present study have identified a far wider variety of oil families than previous surveys, many of which lack diagnostic biomarkers (e.g. botryococcane, bisnorlupanes) which would otherwise conclusively indicate their origin from one or more basins within the Indonesian Archipelago. Ascertaining which varieties of waxy bitumen may be of local origin requires a detailed assessment of the biomarker characteristics of each family in order to compare them with the extremely variable petroleum systems of Indonesia and elsewhere in South East Asia (see Comparison of Waxy Bitumen with Other Datasets). Further work is required before any reliable determination of the origin of these new bitumen families as local or Indonesian can be made.

Whilst the HCA statistical data treatment highlights a geochemical similarity between the fluid inclusions from the Greenly-1 and Gnarlyknots-1A wells to different families of waxy bitumen, comparison of their diagnostic chromatograms (Figure 132 and Figure 133) demonstrates that these similarities are unlikely to be due to sharing a common source because of significant variations in diagnostic compounds.

Comparison of Greenly-1 Fluid Inclusion Geochemistry vs. Type IIID Waxy Bitumen

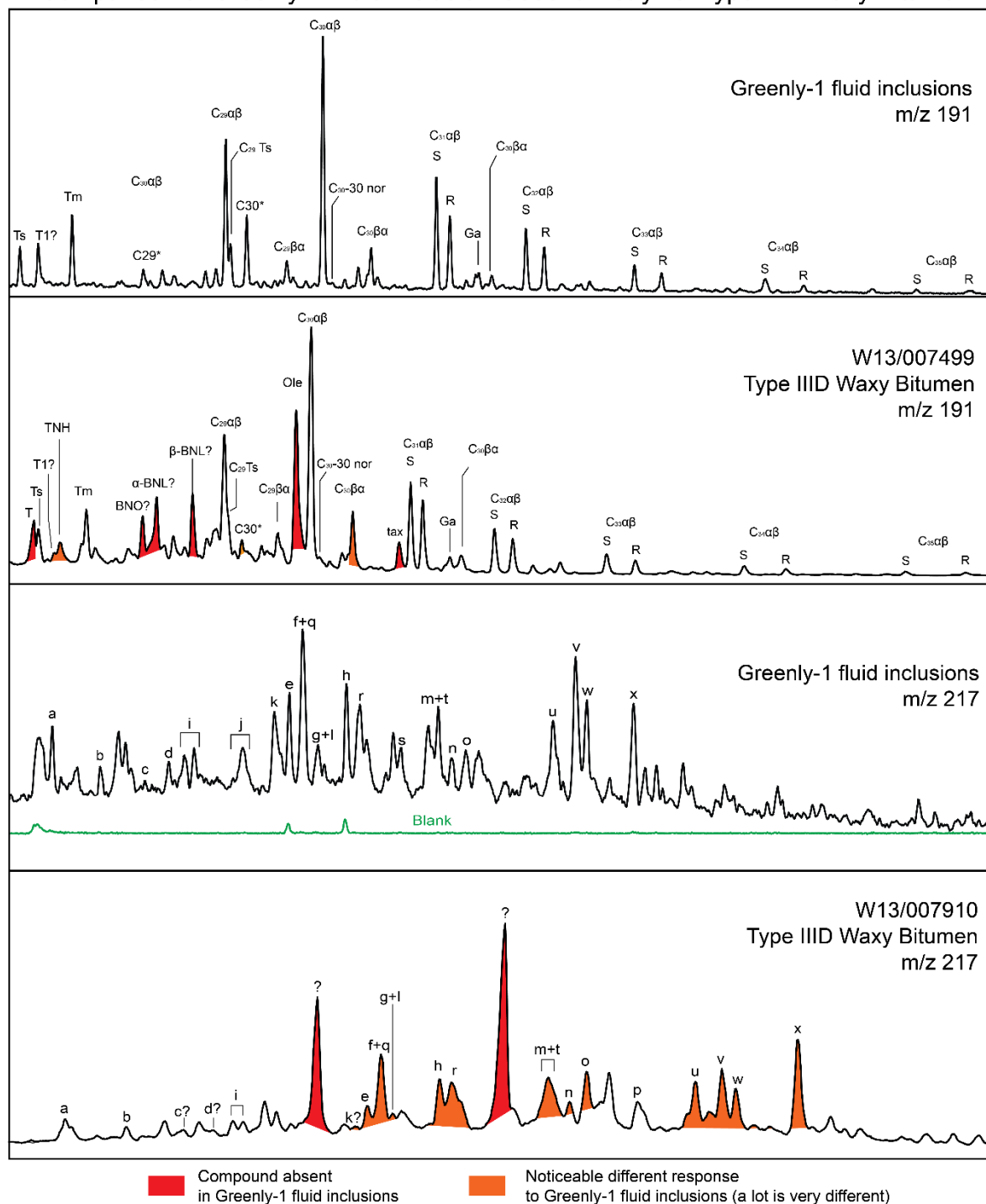


Figure 132: Comparison of the biomarker signatures of Greenly-1 fluid inclusions and Type IIID waxy bitumen (sample W13/007499). Although HCA statistical treatment suggests that this waxy bitumen is comparable to the fluid inclusions from Greenly-1, there are clear differences in their respective alkane compositions which do not support their correlation to the same source.

[illegible]

213

Summary and conclusions

Biomarker analysis of coastal bitumens collected during the GABRP has revealed a previously unidentified complexity in the number petroleum systems which impact the South Australian coastline. Whilst previous surveys identify a total of five families of waxy bitumen (Edwards et al., 2016, 2017), the results presented here distinguish a total of 15 varieties on the basis of their source-specific biomarker geochemistry.

With the identification of multiple previously undocumented oil families, a detailed comparison of their geochemistry against known petroleum systems is required to assess their origin. In particular, the new varieties of waxy bitumen must be assessed for the viability of either their Indonesian provenance or their origin from one of the basins along Australia's margin including the North West Shelf, Perth Basin and the Bight Basin (see Comparison of Waxy Bitumen with Other Datasets). This work is underway and will be included in Alex Corrick's PhD thesis.

Statistical treatment of specific compound ratios from analysed samples shows distinct clustering which corresponds well to families defined by diagnostic biomarkers. While the comparison of this dataset to oils collected from fluid inclusions in the Greenly-1 and Gnarlyknots-1A wells in the GAB suggests minor correlation, assessment of the full suite of diagnostic biomarkers reveals substantial differences in composition which do not support their correlation to a common source. This does not preclude the potential for a local origin for certain families of newly identified bitumen. However, it does suggest they are not directly related to the same petroleum system responsible for the fluid inclusions analysed as part of Theme 5.3.

DEGRADATION OF OIL FAMILIES

The need to define the extent of degradation in coastal bitumen

Oil family identification:

The oil family classification scheme for South Australian coastal bitumen defined in this report is based on the presence and/or absence of specific compounds. In order to recognise the fresh counterparts of a degraded bitumen it is necessary to outline how each of these oil families responds to increasing degradation. This prevents redundant oil families being proposed based on the wide variety of degradation states identified.

Oceanographic provenance modelling:

Hydrocarbons emitted from seafloor seeps are among the most persistent forms of petroleum in the marine environment (Ocean Studies Board and Marine Board, 2003). The bitumen formed from such crude oil has been noted to survive for several months to over a year (Blumer et al., 1973; Butler et al., 1976). As the bitumen is continuously exposed to the wide variety of degradation processes that operate in the ocean and the coastal environment, the extent of its degradation may be considered a proxy for exposure time.

The compounding errors in backtracking the path of bitumen samples using oceanographic models requires that the models "rewind" the bitumen traversal through the ocean currents as little as possible to obtain a meaningful result. Hence, a model tracking bitumen transportation for a year

certainly does not record the sample's true location at the end of the model. Additionally, oceanographic models are not able to simulate an individual bitumen being stranded, washed back to sea and subsequently re-stranded elsewhere. Such a scenario is common in the case of coastal bitumen strandings. Therefore, the specimens used in oceanographic provenance modelling should be selected based on the assumptions that they have washed ashore for the first time, and as recently as possible – assumed to be the day of collection. In practical terms, this means that to provide the oceanographic models with the most reliable input data possible and thereby obtain a meaningful result, only the freshest examples from each oil family must be used

Historical continuity

Comparing recently collected coastal bitumens to their historical counterparts permits an assessment of how their environmental impact has changed through time, thereby providing insight into potential seep behaviour and their relevance (or lack thereof) to recent drilling activity or oil spills.

Introduction to hydrocarbon degradation

The volume of petroleum released into the marine environment from natural seeps alone could cover the oceans of the world in a layer of oil 20 molecules thick (Head et al., 2006). However, following their release from a seafloor seep, hydrocarbons are exposed to a wide variety of degradation processes which lead to their removal, thereby, preventing the aforementioned scenario from occurring. These processes include evaporation, photo-oxidation, water washing and biodegradation (Munoz et al., 1997; Gagnon et al., 1999; Mazeas & Budzinski, 2002; Mazeas et al., 2002; Wenger & Isaksen, 2002; Peters et al., 2005; Fernandez-Alvarez et al., 2007; Wardlaw et al., 2008; Farwell et al., 2009). Collectively these physical and chemical changes may be referred to as “weathering”.

The rate of weathering is situationally dependent. Petroleum composition, ocean temperature, level of exposure to ultraviolet light, total surface area and many other factors ultimately affect the rate at which a crude oil will degrade. These weathering processes preferentially affect different compounds and may occur at differing rates. However, the range of compounds affected may overlap. As a result, it is usually not possible to differentiate or quantitatively define the relative influence of each weathering process in a degradation assessment. Most published studies of hydrocarbon degradation are focused on alteration in the reservoir or, in the case of oil spills, at the ocean surface. In both instances degradation is concentrated along an oil-water contact. Oil spills quickly form a thin film on the sea surface. With a large surface area in contact with seawater and exposure to sunlight, the oil may become extremely degraded within hours to days. The rate at which weathering processes affect liquid petroleum in the marine environment is not directly comparable to the weathering of semi-solid bitumen in the water column which is slower, because its smaller surface area limits the rate of alteration. This results in bitumen having a substantially longer lifespan in the ocean than does liquid petroleum.

Assessment of the extent of weathering of coastal bitumen directly attributable to its exposure to the marine environment is further complicated by the fact that the parent oil may have undergone water washing and biodegradation in the subsurface before being re-exposed to different varieties of these same processes upon entering the ocean.

Biodegradation

With respect to petroleum, biodegradation is defined as the alteration of crude oil by living organisms (Milner et al, 1977; Connan 1984; Palmer 1993 and Blanc & Connan, 1992). A review by Prince (2005) notes 79 bacterial genera, 103 fungal genera and 14 algal genera which are known to degrade hydrocarbons. Typically, biodegradation is limited by available nutrients, predominantly nitrogen and phosphorus (Atlas & Bartha, 1972), rather than the amount of biodegrading microorganisms, which may grow and multiply rapidly if provided with a source of hydrocarbons.

Biodegradation predominantly results in the loss of saturated and aromatic hydrocarbons, and a concomitant increased abundance of more recalcitrant polar compounds (Head et al., 2006). Normal alkanes in the C₁₀-C₂₄ range degrade most rapidly, while higher molecular weight homologues are more resistant to biodegradation (Peters et al., 2005). However, because the microorganisms which degrade hydrocarbons reside in water, water washing and biodegradation occur simultaneously (Palmer 1984, 1993). Therefore separating the effects of biodegradation from those of water washing is commonly not possible, particularly when assessing the C₁₅+ fraction (Palmer 1984). As alteration progresses, lighter compounds are catabolised and removed faster than high-molecular-weight compounds, giving rise to the appearance of sequential alteration and selective removal by compound class. However, it is important to realise that all compounds undergo biodegradation simultaneously, albeit at differing rates (Figure 134). As biodegradation and water washing proceed the API gravity of the residual oil decreases and its relative abundance of NSO compounds and trace metals increases (Peters et al., 2005). The effects of biodegradation can be identified in crude oil within hours of contact with water and continue for months to >1 year (Head et al., 2006).

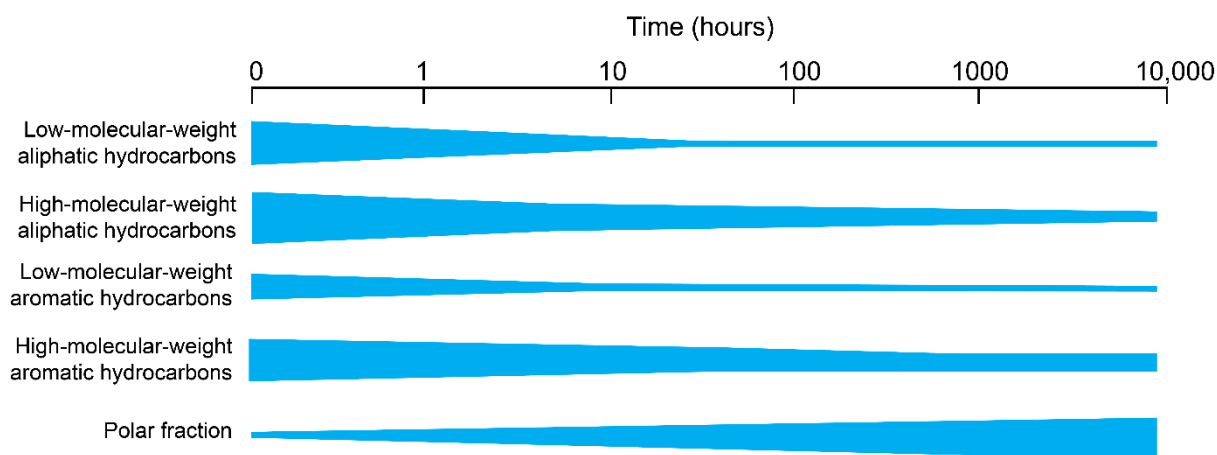


Figure 134: Generalised timeframe for crude oil biodegradation modified after Head et al., (2006). Note that coastal bitumen occupies the right-hand third of this plot.

The rate of biodegradation is not uniform in all cases. Biodegradation occurs as a function of multiple factors including the composition of the crude oil, surface area in contact with water, type of microorganisms present, nutrient availability and, when occurring in the reservoir, characteristics such as grain size, lithology, porosity, permeability and temperature of the host rock. Additionally, because the parent petroleum systems for each of the varieties of coastal bitumen have not been explicitly located and characterised, any alteration which may have occurred in the reservoir cannot

be separated from that which ensued following release of the parent oil into the marine environment.

Despite the inherent variability associated with biodegradation, numerous classification schemes have been proposed that may be used to broadly characterise the extent of alteration based on the removal of specific compounds. Two of the most commonly used biodegradation scales are those of Wenger et al., (2002) and Peters & Moldowan (1993), summarised in Figure 135.

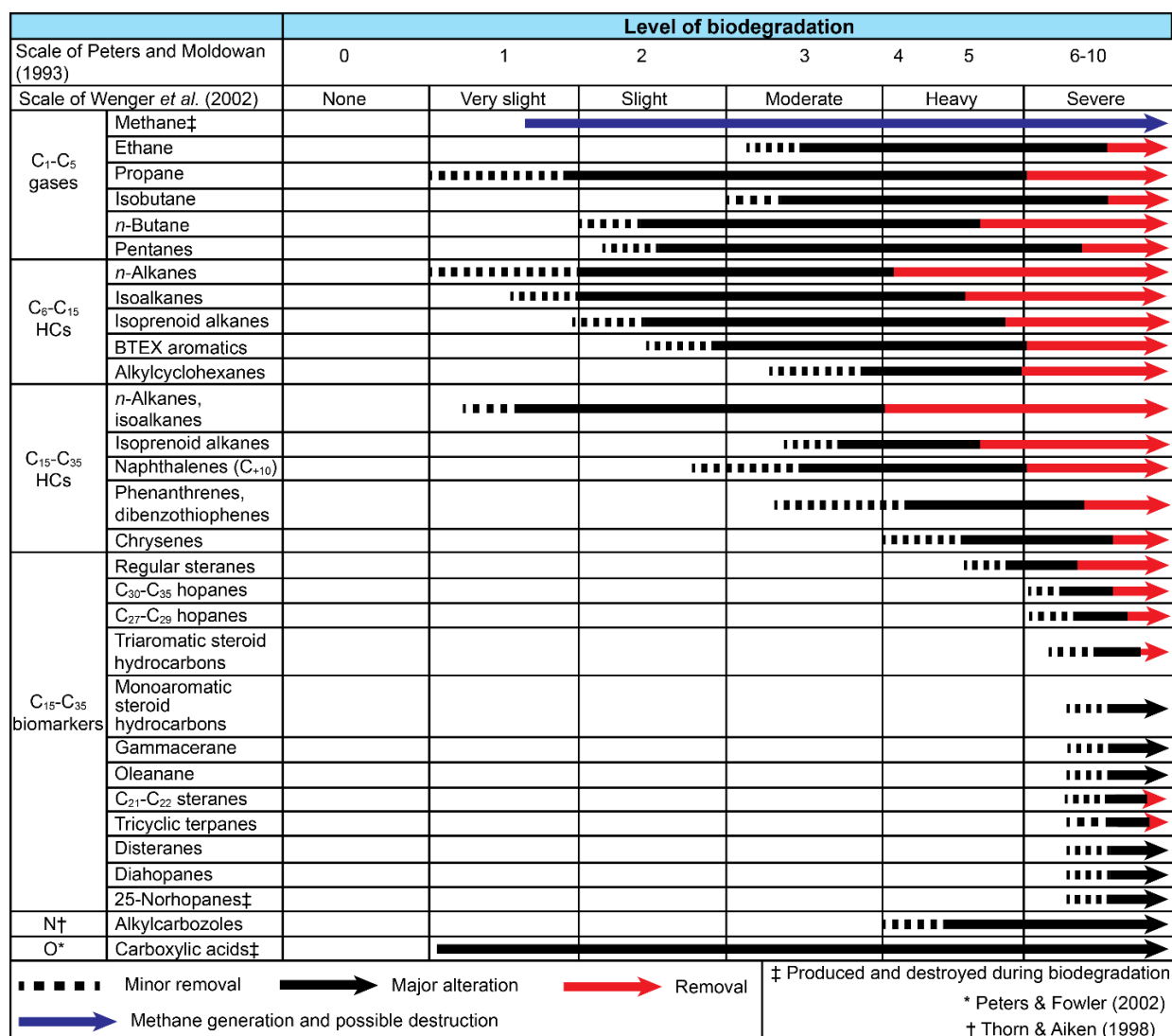


Figure 135: Summary of the Wenger et al., (2002) and Peters & Moldowan (1993) biodegradation scales. Figure modified after Head et al., (2003). Note that this is a generalised classification system subject to variation on a case-by-case basis.

Water washing

Many compounds found in petroleum are soluble in water to differing degrees (McAuliffe, 1966). Exposure to seawater (or invasion of the reservoir by groundwater) therefore may result in the selective removal of the more soluble components. As mentioned previously, water washing is

commonly accompanied by biodegradation, as the seawater/groundwater hosts the microorganisms responsible for biodegradation.

The generalised sequence of removal according to compound class and its relative aqueous solubility is: aromatic hydrocarbons > cycloalkanes > branched alkanes > *n*-alkanes (Palmer, 1984; 1993; Lafargue & Barker, 1988; Kuo, 1994; Lafargue & Le Thiez, 1996). With respect to the *n*-alkanes, water washing is most effective at removal of the gasoline (C₅-C₁₀) and kerosene (C₁₁-C₁₃) range homologues, for which solubility decreases with increasing molecular weight.

Evaporation

Evaporation is one of the dominant weathering processes responsible for the dissipation of oil slicks (Ocean Studies Board & Marine Board, 2003), largely removing their low-molecular-weight (<C₁₅) components (Peters & Moldowan, 2005). The initial composition of the spilled oil determines the volume of hydrocarbons which may be lost via evaporation. Light crude oils may lose up to 75% of their initial volume, while medium and heavy/residual crudes may lose up to 40% and <10%, respectively, after several days.

While evaporation is arguably as important as biodegradation in the breakdown of surficial oil slicks, the inspissated and semi-solid nature of coastal bitumen means that it has already lost most of its volatile components. Hence, the effects of evaporation are less significant and likely restricted to the specimen exterior.

Photo-oxidation

When exposed to the ultraviolet to near-ultraviolet range of the sunlight spectrum, crude oil will undergo photo-oxidation (Lee, 1980 and references therein). The products of photo-oxidation include carboxylic acids, alcohols, ketones, phenols and aldehydes (Lee, 1980; Sanniez & Pinckney, 1978; Larson et al., 1979; Ehrhardt & Weber, 1995; Ehrhardt et al., 1997; Ehrhardt, 1987; Hansen, 1975). These compounds have high aqueous solubility and are subsequently removed by water washing (Hansen, 1975; Larson et al., 1976; Lee 1980). Whilst saturated hydrocarbons (alkanes) are resistant to photo-oxidation, aromatic hydrocarbons are easily altered (Garrett et al., 1998). As freshly spilled oil rapidly disperses in a thin film on the sea surface, its resulting high surface area to volume ratio makes photo-oxidation a significant contributor to hydrocarbon alteration. However, in the case of semi-solid bitumen, this ratio is much lower and therefore such alteration may only affect the exposed surface of the specimen.

Asphaltite Degradation

Visual and physical characteristics of degradation

Asphaltites display very little visual evidence of degradation. All asphaltites contain deep shrinkage cracks and the exterior shows no change in colour with increasing alteration. The freshest asphaltites are among the largest collected and possess a soft and pliable interior. However, as asphaltites degrade they become increasingly brittle and may break apart into smaller pieces that exhibit a distinctive conchoidal fracture (Figure 136).

(A)

W13/007477



(B)

W13/007664

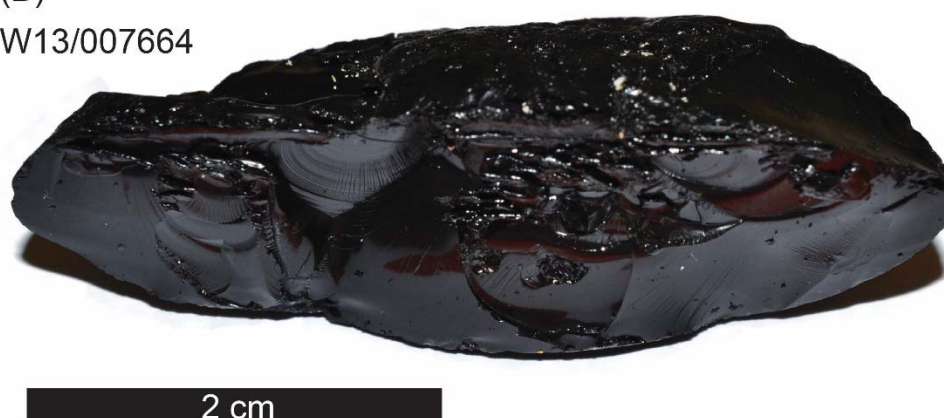


Figure 136: Asphaltites displaying characteristic conchoidal fractures. (A) Sample W13/007742, a typical asphaltite. (B) Sample W13/007664, a highly degraded asphaltite collected from Tractor Beach.

Approach to degradation assessment

As the asphaltites have been interpreted to originate from local seafloor seeps (Hall et al., 2014), a full suite of analyses has been undertaken to characterise their degradation in order to determine the best system for identifying the freshest samples. This included whole-oil GC-MS screening, GC-MS analysis of the saturated and aromatic hydrocarbon fractions and compound-specific isotope analysis (CSIA) of the *n*-alkanes.

Whole oil GC-MS

The range of degradation states identifiable in asphaltite samples using whole-oil GC-MS screening is shown in Figure 137. Most asphaltites collected between 2014 and 2016 are lightly biodegraded,

comparable to sample W13/007507. Specimens as fresh as W13/007976 and as degraded as W13/007566 are exceptions to the norm. The former, the largest asphaltite found during the beach surveys, was collected following heavy storm activity immediately prior to the survey, while the latter was recovered not from a stranding location on the beach but from the eroded remains of an established dune system. The most degraded asphaltites, such as sample W13/007664 which were only encountered on Tractor Beach and represent outliers among the asphaltite collection. These bitumens are identified as asphaltites on the basis of their visual features including their diagnostic conchoidal fracture, but geochemically are heavily biodegraded beyond straightforward recognition.

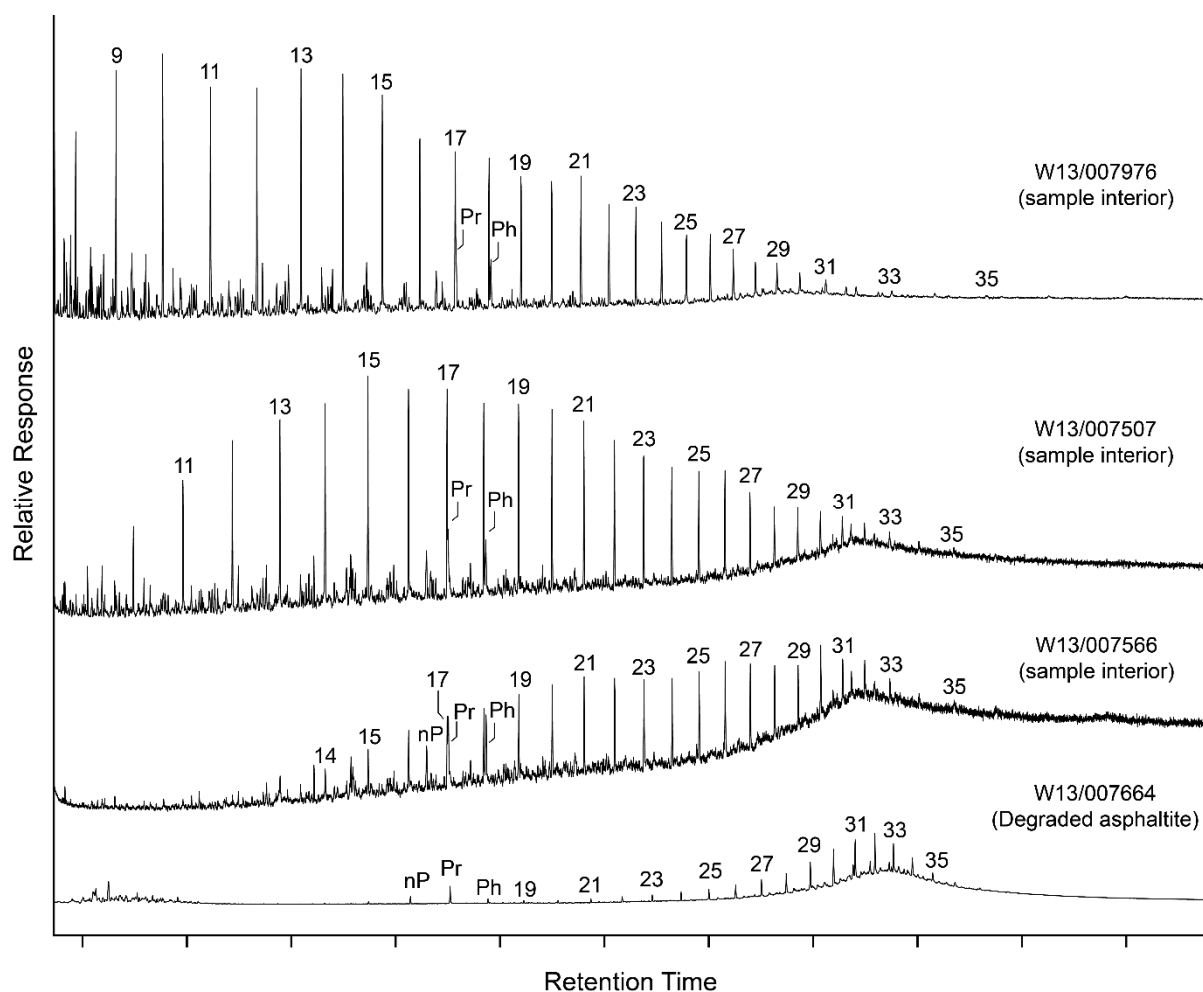


Figure 137: Variation in whole-oil GC-MS chromatograms of asphaltites attributable to weathering. Each chromatogram is scaled such that no compound which is not a product of biodegradation may have a higher response than the freshest sample. Most of the asphaltites collected are comparable to the slightly biodegraded sample W13/007507. The unusually fresh (sample W13/007976) and highly weathered (sample W13/007566) specimens are rare exceptions. Sample W13/007664 is an example of the highly degraded asphaltite specimens found only at Tractor Beach. These highly degraded samples required analysis using a splitless injection (no dilution) in order to resolve the remaining hydrocarbons, which are present in extremely low abundance.

Historical continuity

Previous surveys identified a small range of biodegradation states in asphaltites (Padley, 1995). The new suite of samples collected between 2014 and 2016 has expanded this range with new examples for the freshest asphaltite analysed (W13/007976), and the most heavily degraded (highly degraded asphaltites collected from Tractor Beach).

The continued stranding of fresh asphaltites supports previous interpretations that they are not the result of anthropogenic pitch used historically to seal whaling ships. In addition, the presence of such fresh examples suggests minimal exposure to the marine environment, supporting the interpretation that the asphaltites are of a local origin in the Bight Basin.

Compound Specific Isotope Analysis

Carbon isotopic composition of individual n -alkanes

The recent investigation by Hall et al., (2014) proposed that differences in the $\delta^{13}\text{C}$ values of individual n -alkanes between the exterior and interior portions of asphaltite specimens could be used to provide a degradation assessment.

To test the validity of this approach, four large asphaltites were sampled in cross-section (Figure 138) to assess their geochemical variability. The viability of applying CSIA data as a proxy for weathering relies on the fundamental assumption that the samples were isotopically homogeneous when fresh, and that any variability is thus result of degradation processes. Thus, the exterior of any given specimen should display the largest difference when compared to the interior.

The difference between the interior and exterior values of $\delta^{13}\text{C}$ for each individual n -alkane ($\text{C}_{13}\text{--}\text{C}_{35}$) is shown in Figure 139 (all CSIA stored in Appendix 7). Whilst specimen exteriors were most frequently enriched in ^{13}C compared to the interior, sub-samples collected in between the exterior and interior (“mid” samples) show even greater variability, producing highly inconsistent trends. In addition, the range of variability is often within the range of compounded experimental error associated with the data collection.

As the asphaltite exterior may not be the most geochemically distinct part of an asphaltite when compared to its centre, this brings into question the assumption that such variability is predominantly a function of weathering. Rather, the asphaltites themselves may be isotopically heterogeneous or the experimental error associated with the data collection results in inaccurate trends. Therefore, whilst weathering may influence the isotopic composition of n -alkanes in asphaltites, these results demonstrate that CSIA is not a viable weathering assessment tool.

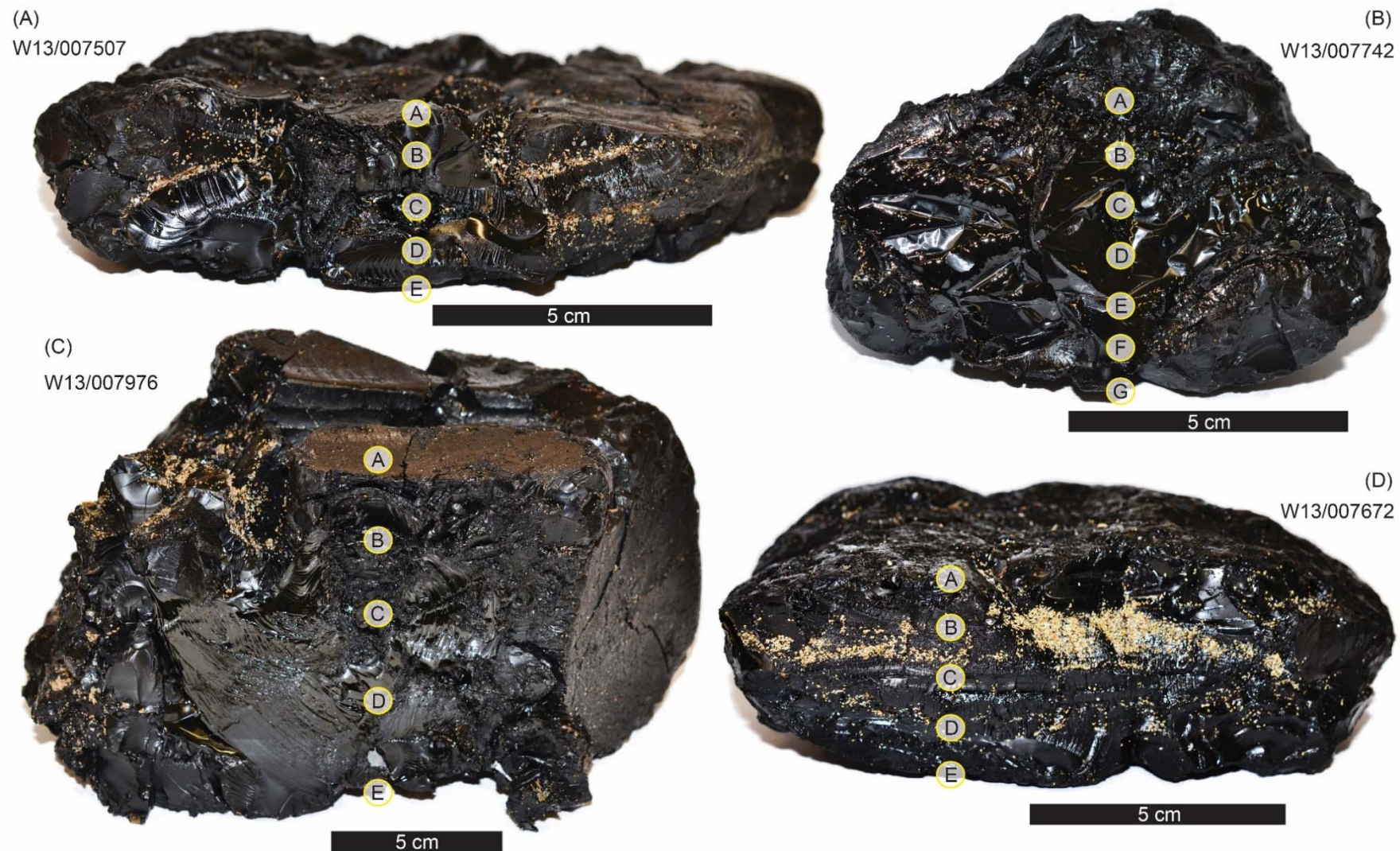


Figure 138: Asphaltites sub-sampled in cross-section to assess variability using CSIA. Sampled locations marked on each specimen (A) Sample W13/007507. (B) Sample W13/007742. (C) Sample W13/007976. (D) Sample W13/007672.

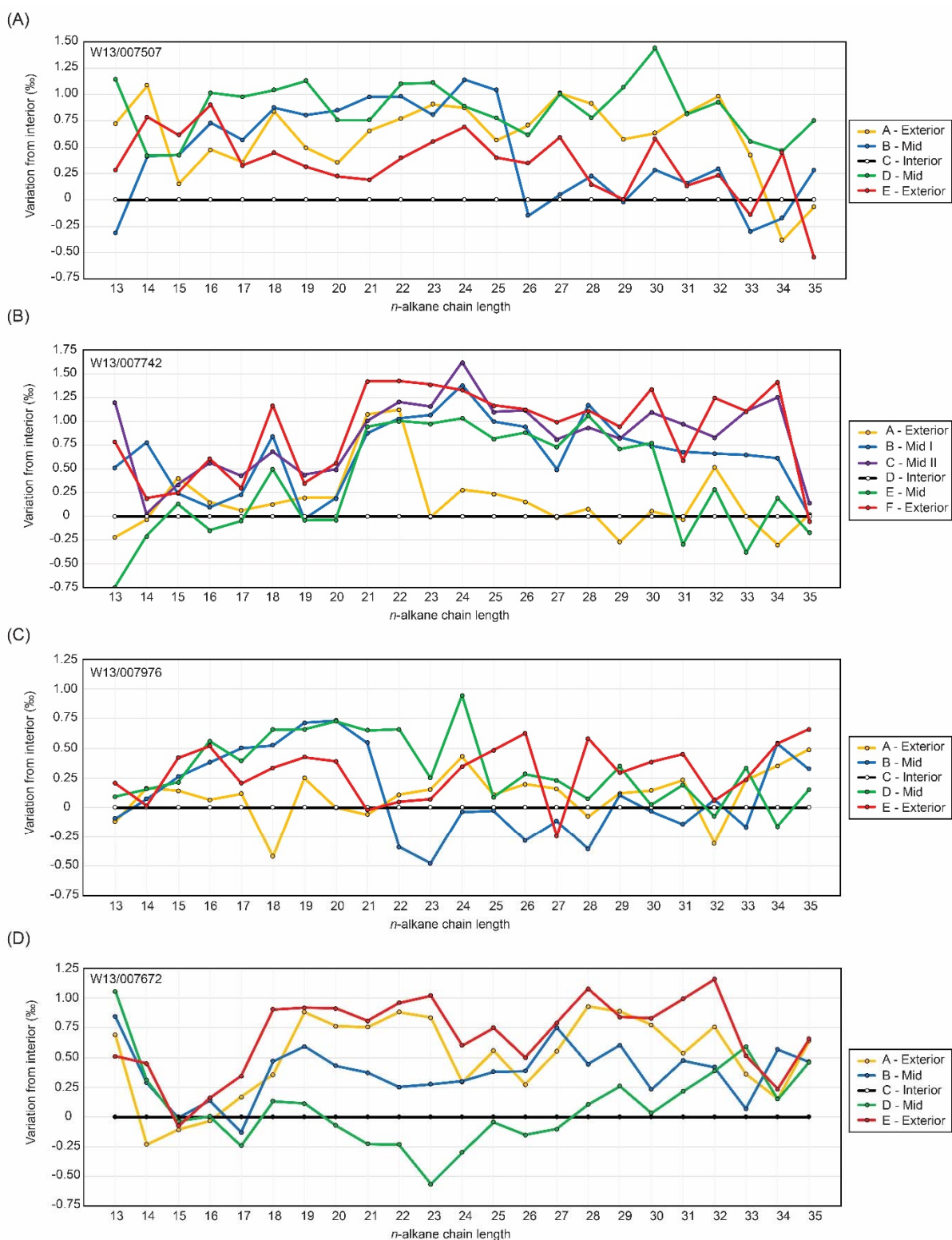


Figure 139: Difference in the carbon isotopic composition of individual *n*-alkanes of asphaltite sub-samples compared to the specimen interior. (A) Sample W13/007507. (B) Sample W13/007742. (C) Sample W13/007976. (D) Sample W13/007672.

Asphaltite Biomarker Degradation Assessment

Almost all asphaltites collected between 2014 and 2016 show negligible variation in their biomarker composition due to their low levels of biodegradation. However, the highly degraded asphaltites collected from Tractor Beach in 2015/2016 (e.g. W13/007664) show extensive alteration and complete removal of many of the biomarkers commonly used in source interpretation and oil-oil correlation.

Traditionally, the C_{27} - C_{30} $\alpha\alpha\alpha$ 20R steranes (labelled h, n, p and x, respectively in Figure 140) are considered the most susceptible to biodegradation and therefore the first to undergo alteration. This alteration sequence has been described in field studies (Rullkötter & Wendisch, 1982; Seifert et al., 1984; Landais & Connan, 1986), oil spill studies (Mille et al., 1998; Wang et al., 2001) and bacterial culture experiments (Goodwin et al., 1983; Chosson et al., 1991).

Comparisons of the biomarker signatures of increasingly degraded asphaltites are shown in Figure 140 and Figure 141, where alteration and removal of compounds appears to occur largely as a function of increasing carbon number. Most notably, these samples show unorthodox biodegradation in their sterane / diasteranes composition, including the rapid removal of C_{27} $\beta\alpha$ diasteranes (labelled a and b in Figure 140), C_{27} $\alpha\beta\beta$ steranes (labelled f and g in Figure 140). Traditionally, diasteranes are considered extremely resistant to biodegradation, with studies of other oils suggesting alteration of diasteranes begins only after complete removal of the C_{27} - C_{29} steranes (Seifert & Moldowan, 1979; McKirdy et al., 1983; Seifert et al., 1984; Connan, 1984; Requejo et al., 1989). Inspection of the m/z 191 chromatogram (Figure 141) also reveals complete removal of tricyclic terpanes, severe alteration of the maturity-sensitive C_{27} triterpanes Ts and Tm, and extensive drawdown of the C_{29} - C_{35} $\alpha\beta$ hopanes. As noted previously, these highly degraded samples were only collected from Tractor Beach and represent outliers to the range of degradation evident in the asphaltite dataset. However, care should be taken to recognise these examples as extremely degraded asphaltites. This may prevent misclassification as a separate oil family with different source-specific biomarker ratios, which are the result of alteration rather than features inherited from the source rock.

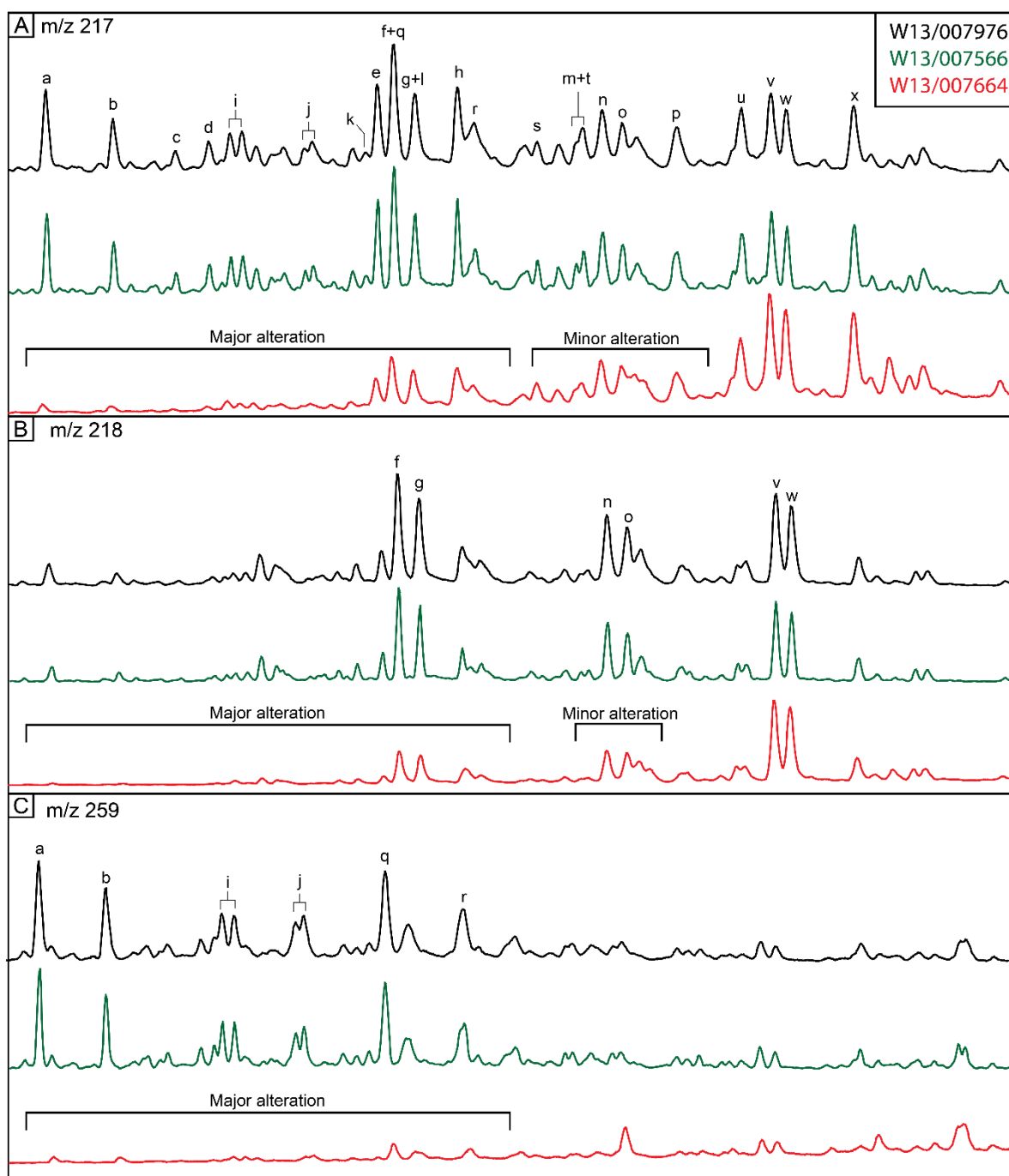


Figure 140: Assessment of sterane and diasteranes degradation in asphaltites. Each chromatogram is scaled such that no compound which is not a product of biodegradation may have a higher response than the freshest sample. Selected samples include the freshest asphaltite (W13/007976), a moderately biodegraded asphaltite (W13/007566) and a highly degraded asphaltite (W13/007663). (A) Sterane and diasteranes degradation identified in m/z 217. Co-eluting compounds are separated in later sections (B) Steranes ($\alpha\beta\beta$) degradation identified in m/z 218. (C) Diasterane ($\beta\alpha$) degradation identified in m/z 259. For peak identifications refer to table 19.

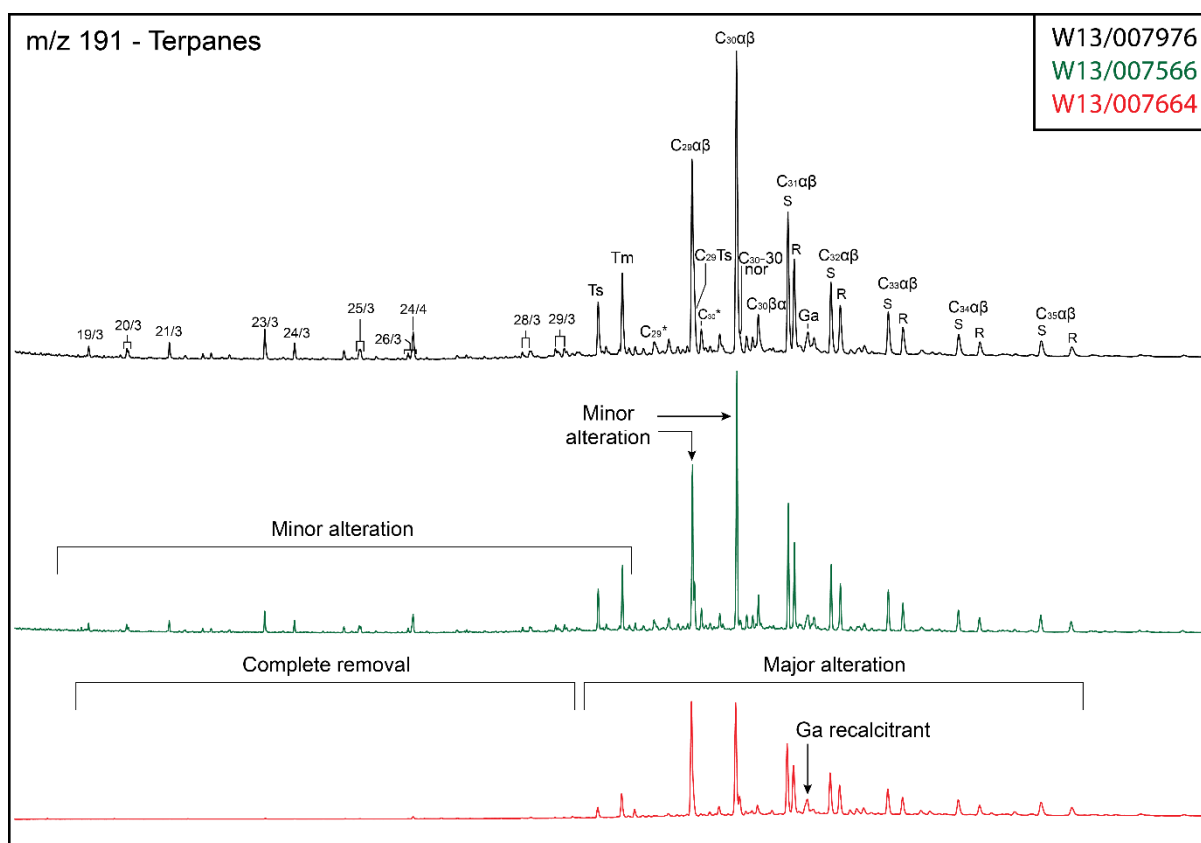


Figure 141: Assessment of the degradation of terpanes in asphaltites in the m/z 191 chromatogram. Each chromatogram is scaled such that no compound which is not a product of biodegradation may have a higher response than the freshest sample. Fresh to moderately degraded samples (W13/007976 and W13/007566) show minimal alteration of biomarkers. In heavily degraded examples such as W13/007664, many components are lost and others severely altered. For peak identifications refer to table 18.

Degradation of waxy bitumen

Waxy bitumens comprise the majority of the bitumen samples collected from the South Australian coastline and exhibit a wide range of degradation states. Each whole-oil family was assessed individually to identify the full range of degradation states, from freshest to most degraded.

Visual and physical characteristics of degradation

Highly weathered waxy bitumen may develop a brown and brittle exterior (Figure 142). However, this is not guaranteed in all cases, and highly degraded examples may also remain black. Instances of waxy bitumen browning are attributed to a greater proportion of weathering from oxidation and degradation in sunlight compared to water washing and biodegradation. A visual/physical assessment of the bitumen alone is therefore not an adequate weathering assessment which requires a geochemical approach.

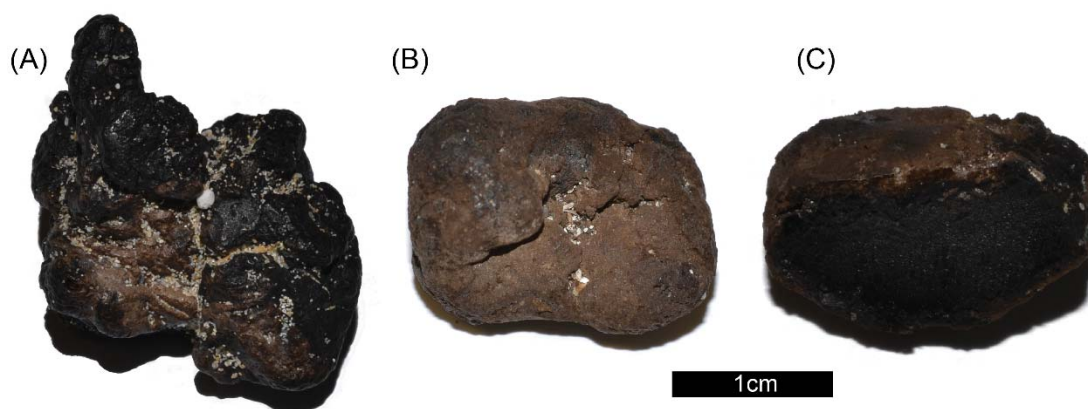


Figure 142: Examples of surficial browning of waxy bitumen associated attributable to weathering:
(A) Sample W13/007625 exhibiting partial browning. (B) Sample W13/007521, a highly degraded waxy bitumen with an entirely brown and brittle exterior. (C) Sample W13/007521 in cross-section, highlighting that browning is restricted to its exposed exterior.

Approach to degradation assessment

Interior vs. exterior geochemical comparison

Guided by the previous work of Hall et al., (2014) on coastal asphaltites, a geochemical comparison of the interior and exterior portions of individual tarballs (waxy bitumen) was considered a potential metric for their degree of weathering. However, the results proved too inconsistent to provide a reliable assessment. This was due to a wide range of variation in the level of degradation of the interior from sample to sample (Figure 143). The range of degradation states within the interiors of the collected waxy bitumen do not allow for a consistent geochemical baseline to be established for comparison with their respective exteriors, making the extent of variation between interior and exterior an unreliable assessment of the overall extent of degradation. This high degree of variation is attributed to microbial activity penetrating the waxy bitumen to a greater extent than anticipated based on historical data. As the sample interiors were found not to be consistent, the magnitude of variation between the interior and exterior is not a reliable measure of overall weathering that allows samples of the same oil family to be ranked according to their degree of alteration.